Chapter 3

TROPICAL CYCLONE FORMATION

John L. McBride

[Based in part on Chapter 3 of *A Global View of Tropical Cyclones* by W. M. Frank. This chapter is also greatly influenced by discussions over many years with W.M. Frank, W.M. Gray, Klaus Fraedrich, G.J. Holland, N.E. Davidson, T.D. Keenan, and K.K. Puri.]

3.1 INTRODUCTION

Tropical cyclones form from initial convective disturbances known as cloud clusters. As they evolve from a loosely organized state into mature, intense storms, they pass through several characteristic stages. As described in Chapter 1, a uniform terminology does not exist to describe these stages over the different regions of the globe. General agreement exists that a key stage in the formation process is when the system reaches sustained surface winds exceeding 17.5 m s^{-1} (34 kt). In this chapter, such systems are referred to as *tropical cyclones*. Another agreed threshold is sustained surface winds of 33 m s^{-1} (64 kt), which will be referred to in this chapter as *severe tropical cyclones* (synonymous with *typhoons* in the western North Pacific and *hurricanes* in the Atlantic and eastern Pacific).

As described in Chapter 2, the mature tropical cyclone has a characteristic structure on two horizontal scales. The large-scale tropospheric vortex may extend over 1000-2000 km from the region of minimum surface pressure at the center. On this scale, the wind and the mass fields are in approximate gradient balance through the depth of the troposphere. Since the thermal structure has a warm core in the upper troposphere, thermal wind considerations require that the strength of the vortex decreases rapidly with height in the upper troposphere, and on the larger scale turn anticyclonic (Fig. 2.2). Embedded within this large-scale circulation is the region containing the eye, the eyewall cloud, and the central core of maximum winds. The horizontal extent of the core is on the order of 100 km. This central (or core) region has the same basic thermal structure, but is characterized by very large horizontal gradients in comparison to the large-scale system. The characteristic horizontal pressure gradients are of the order of 1 mb km^{-1} (as compared with approximately 0.01 mb km^{-1} for the larger scale envelope). In the core, the wind magnitudes are such that the balance is approximately cyclostrophic rather than gradient (Fig. 2.12).

The existence of the two horizontal scales has presented semantic difficulties. Various author's use of terms such as "genesis," "formation," and "development" is dependent on the analysis method, data base, and objective of each study. Generally, the existence of a core region can be identified with the time that the system is classified as a tropical cyclone (i.e., wind speeds exceeding 17.5 m s^{-1}). Further development of the maximum wind speeds beyond 17.5 m s^{-1} is referred to as *intensification*. This stage includes the evolution of the core into a well-defined radar eye. Although the larger scale (i.e., thousand kilometer) vortex already exists when the core develops, much of the research into tropical cyclone formation has examined the formation of this large-scale vortex.

The distinction between core formation and large-scale vortex formation is important because different dynamical processes may be involved. From angular momentum considerations, an increase of the rotational wind speed of the core may be accomplished by an import of angular momentum from the surrounding regions. Because the radius of the core region is small, large increases in core wind speeds may occur from only small changes in the large-scale vortex. Consider an increase of core angular momentum commensurate with a tangential wind change (Δv_T) of 10 m s^{-1} averaged over the inner 100 km. Defining relative angular momentum as rv_T, then the average angular momentum increase is (2/3)(100 km)(10 m s^{-1}) multiplied by the area (100 km)^2. If it is

assumed the increase was extracted from the annulus between 100 and 200 km radius, then dividing by the area and average radius of that annulus yields a decrease in tangential winds of only 1.4 m s^{-1}. If it had come from the 100 to 300 km annulus, the average wind decrease would be only 0.4 m s^{-1}. Thus, large changes in magnitude of winds in the core (intensification) may occur relatively independently of changes in the outer vortex winds (referred to as strength and/or size changes in Fig. 2.13b).

In summary, *tropical cyclone formation* in this chapter will simply refer to the transition from the cloud cluster state to the tropical cyclone stage with winds exceeding 17.5 m s^{-1}. Further changes in the maximum wind speed will be referred to as intensification. Changes in wind speed of the outer vortex will be referred to as outer structure change, or strength change, or size change. The emphasis in this chapter will be on the processes involved in tropical cyclone formation.

3.2 CLIMATOLOGICAL CONDITIONS FOR TROPICAL CYCLONE FORMATION

Each year approximately 80 tropical cyclones occur throughout the world, and about two thirds of these reach the severe tropical cyclone stage (Table 3.1). Gray (1968, 1975) documented the initial detection points of each cyclone for a 20-year period (Fig. 3.1). Preferred regions of formation are over the tropical oceans. No formations occur within about 2.5° lat. of the equator. Most of the formations (87%) occur between 20°N and 20°S (Fig. 3.2). About two thirds of all cyclones occur in the Northern Hemisphere, and twice as many tropical cyclones occur in the Eastern as in the Western Hemisphere. These differences are due in part to the absence of tropical cyclones in the South Atlantic and the eastern South Pacific.

Table 3.1 Annual tropical cyclone frequency during 1968 through 1989-90 season in seven basins (Neumann 1993), where left (right) entry is the number with maximum sustained surface wind exceeding 17 m s^{-1} or 34 kt (32 m s^{-1} or 64 kt).

Season N.Hem	S.Hem	North Atlantic	Eastern N Pacific	Western N Pacific	North Indian	Southwest Indian <100°E	Australia/ SE Indian 100-142°E	Australia/ SW Pacific >142°E	Totals
1968	1968-69	8(5)	18(6)	27(20)	7(4)*	8(4)*	4(0)*	7(3)*	79(42)
1969	1969-70	18(12)	10(4)	19(13)	6(2)*	13(8)*	4(2)*	7(3)*	77(44)
1970	1970-71	10(5)	19(4)	24(12)	7(4)*	15(10)*	7(6)*	7(3)*	89(44)
1971	1971-72	13(6)	18(12)	35(24)	7(4)*	8(5)*	6(3)*	16(11)*	103(65)
1972	1972-73	7(3)	14(9)	30(22)	7(6)*	13(8)*	8(6)*	10(2)*	89(56)
1973	1973-74	8(4)	12(7)	21(12)	6(1)*	8(1)*	9(6)*	13(3)*	77(34)
1974	1974-75	11(4)	18(11)	32(15)	7(2)*	10(3)*	9(5)*	5(3)*	92(43)
1975	1975-76	9(6)	17(9)	20(14)	7(3)*	8(3)*	8(3)*	11(5)*	80(43)
1976	1976-77	10(6)	15(9)	25(14)	10(4)*	9(5)*	6(5)*	13(3)*	88(46)
1977	1977-78	6(5)	8(4)	19(11)	6(5)*	14(2)*	6(3)*	10(4)*	69(34)
1978	1978-79	12(5)	19(14)	28(15)	6(3)*	9(4)*	7(3)*	8(3)*	89(47)
1979	1979-80	9(5)	10(6)	23(14)	5(3)*	12(5)*	9(7)*	9(4)*	77(44)
1980	1980-81	11(9)	14(7)	24(15)	3(0)*	12(2)*	10(6)*	10(4)*	84(43)
1981	1981-82	12(7)	15(8)	28(16)	6(3)*	11(4)*	11(4)*	2(2)*	85(44)
1982	1982-83	6(2)	23(12)	26(19)	5(4)*	6(0)*	4(1)*	12(10)*	82(48)
1983	1983-84	4(3)	21(12)	23(12)	3(1)*	11(4)*	7(4)*	7(3)*	76(39)
1984	1984-85	13(5)	21(13)	27(16)	3(2)*	8(1)*	10(2)*	8(6)*	90(45)
1985	1985-86	11(7)	23(13)	26(17)	7(0)*	12(5)*	8(2)*	8(5)*	95(49)
1986	1986-87	6(4)	17(9)	27(19)	1(0)*	7(3)	6(3)*	12(6)	75(43)
1987	1987-88	7(3)	20(10)	24(18)	5(1)*	14(7)	1(0)*	7(3)	79(43)
1988	1988-89	12(5)	15(7)	26(14)	3(1)*	12(9)	5(3)*	11(5)	85(45)
1989	1989-90	11(7)	17(9)	31(21)	3(2)*	8(5)*	7(1)*	6(3)*	80(47)
22-year totals		214(118)	364(195)	565(353)	120(55)	228(98)	152(75)	199(94)	1842(988)
Average		9.7(5.4)	16.5(8.9)	25.7(16.0)	5.4(2.5)	10.4(4.4)	6.9(3.4)	9.0(4.3)	83.7(44.9)
Stnd deviation		3.1(2.2)	4.1(3.0)	4.1(3.6)	2.1(1.7)	2.6(2.6)	2.4(2.1)	3.1(2.3)	7.8(6.4)
% Global Total		11.6(12.0)	19.8(19.7)	30.7(35.7)	6.5(5.6)	12.4(9.9)	8.2(7.6)	10.8(9.5)	100.0%

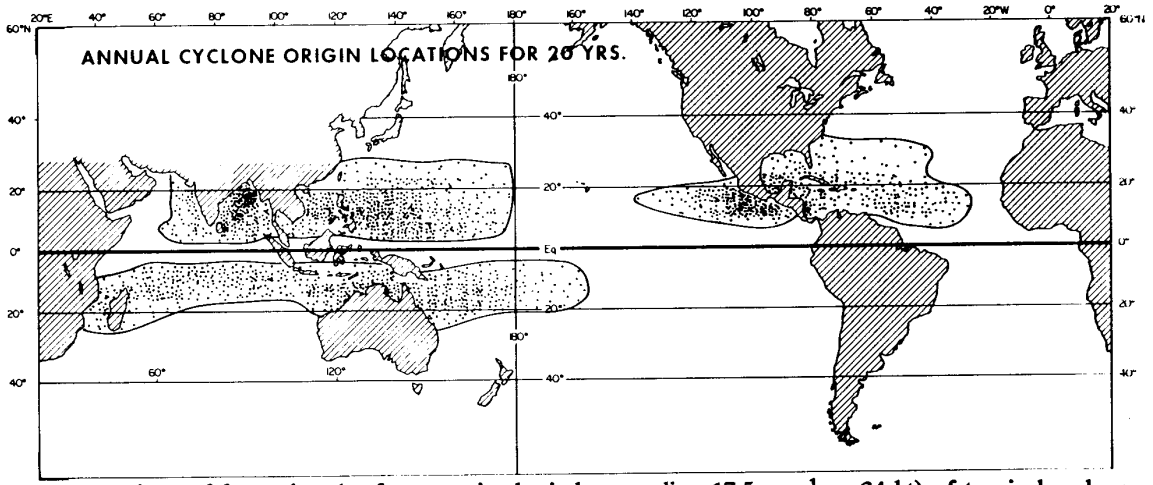

Fig. 3.1 Locations of formation (surface sustained winds exceeding 17.5 m s^{-1} or 34 kt) of tropical cyclone disturbances during a 20-year period (Gray 1975).

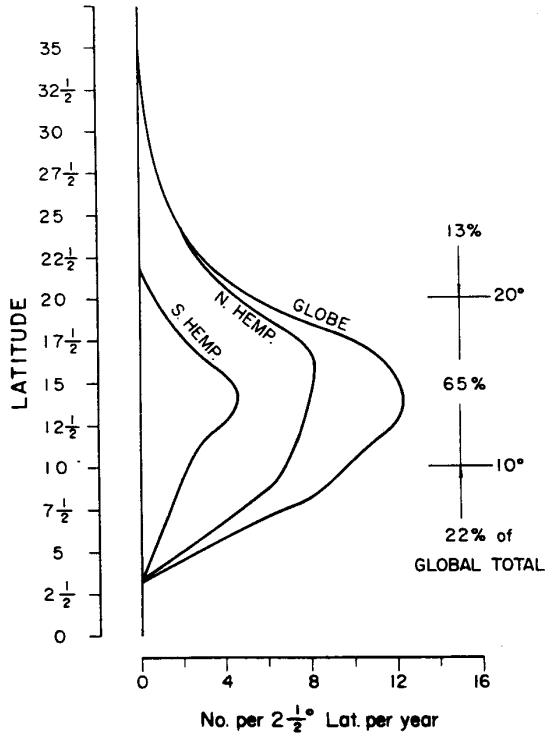

Fig. 3.2 Latitudes at which initial disturbances that later became tropical cyclones were first detected (Gray 1975).

Tropical cyclones are seasonal phenomena, and most basins have a maximum frequency of formation during the late summer to early fall period. The Southern Hemisphere peak occurs in January to March and the Northern Hemisphere peak is from July to September. Neumann (1993) classified the areas of formation into seven "cyclone basins," and updated the previous climatologies for all basins. Intraseasonal aspects of tropical cyclone frequency for each of the seven basins in Table 3.1 will be given later in Fig. 3.9. Combinations of cyclones of all basins are to be presented in Fig. 3.10.

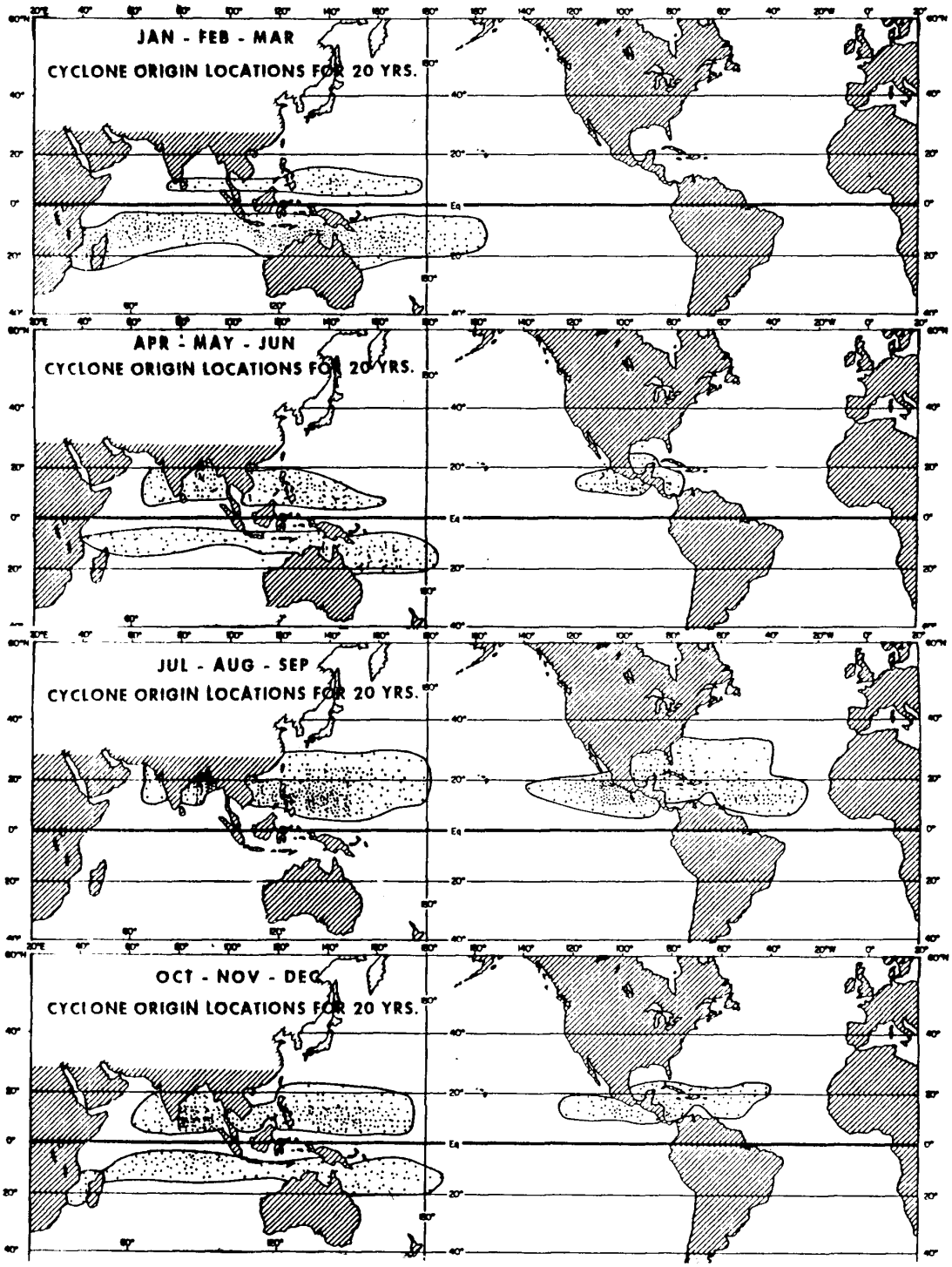

Fig. 3.3 As in Fig. 3.1, except for (a) January-March, (b) April-June, (c) July-September, and (d) October-December (Gray 1975).

The seasonal distribution of formation locations is governed by two major factors. One is the association between tropical cyclone formation and sea-surface temperatures (SST), with the highest values of SST occurring during the late summer. Notice that regions of warm water also extend farther from the equator in the Northern Hemisphere in association with the Gulf Stream and the Kuroshio currents. However, SST is only one factor, as is evidenced by the absence of cyclones in the South Atlantic despite similar values of SST at certain times of the year.

The second factor in the seasonal distributions (Fig. 3.3) is related to the seasonal variations in the location of the monsoon trough. As discussed by Gray (1968), the Inter-Tropical Convergence Zone (ITCZ), which extends semi-continuously around the globe, may occur as a convergence line between trade easterlies from the Northern and Southern Hemispheres, or as a convergence zone in westerly monsoon flow. In this latter configuration, the monsoon westerlies usually have trade easterlies on their poleward side. The shearline separating the monsoon westerlies from easterlies is known as the monsoon trough or monsoon shearline and is a climatologically preferred region for tropical cyclone formation. Typical upper- and lower-level flow patterns for the two modes of the ITCZ are illustrated schematically in Fig. 3.4. The trade convergence line of the ITCZ typically has large vertical wind shear. When monsoon westerlies are present, the low-level monsoon shearline is overlain (in the mean seasonal pattern) by the upper-level subtropical ridge. In western North Pacific, the ridge above the monsoon trough during the summer is called the subequatorial ridge. This configuration of trade easterlies overlain with westerlies and monsoon westerlies overlain with easterlies gives a (seasonal-mean) vertical wind shear close to zero, with westerly shear on the poleward side and easterly shear on the equatorward side (bottom panel, Fig. 3.4).

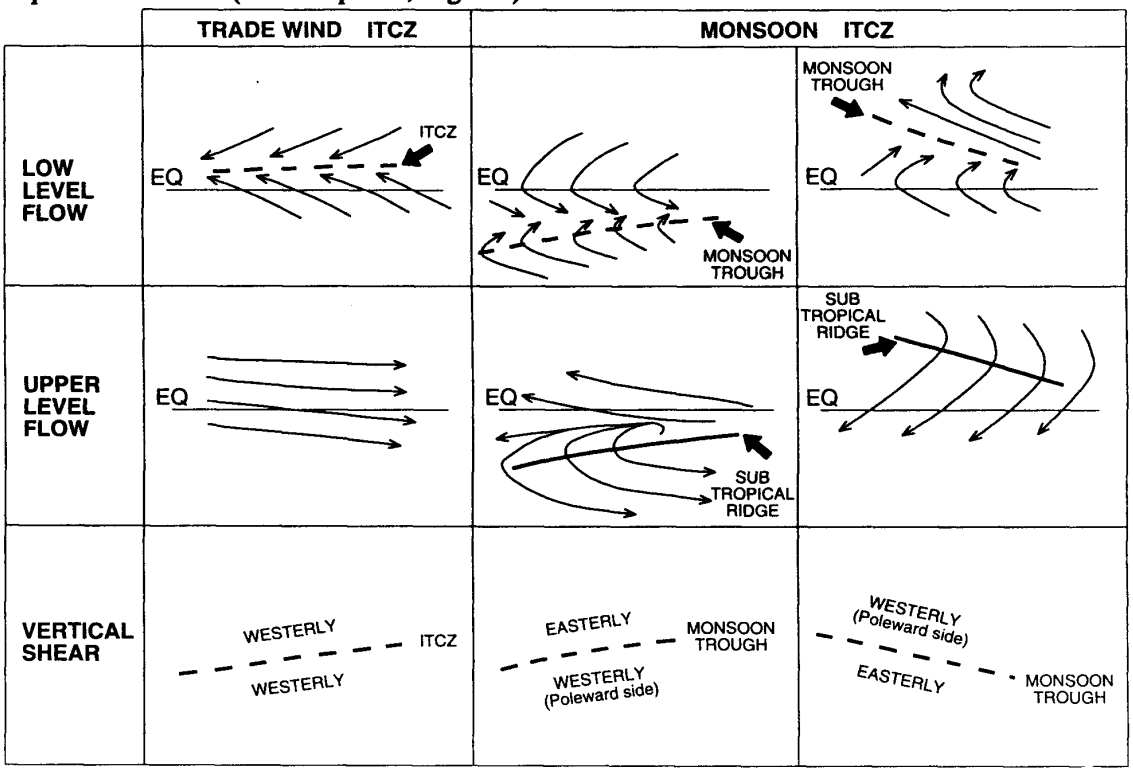

Fig. 3.4 Schematics of tradewind (left) and monsoon-type (right) ITCZ flow regimes typical of the Australian/Southeast Indian Ocean ITCZ during January (middle) and typical of the western North Pacific basin during August (right). Vertical wind shear between the low-level and upper-level flow is indicated in the lower panels.

The seasonal distribution of the mean locations of monsoon-type ITCZs occurring over the oceans is plotted in Fig. 3.5. The association between the monsoon trough and occurrences of tropical cyclones in Fig. 3.3 is quite marked. The only region of cyclone formation not associated with a monsoon trough is the North Atlantic. Possible explanations for this anomaly will be discussed later.

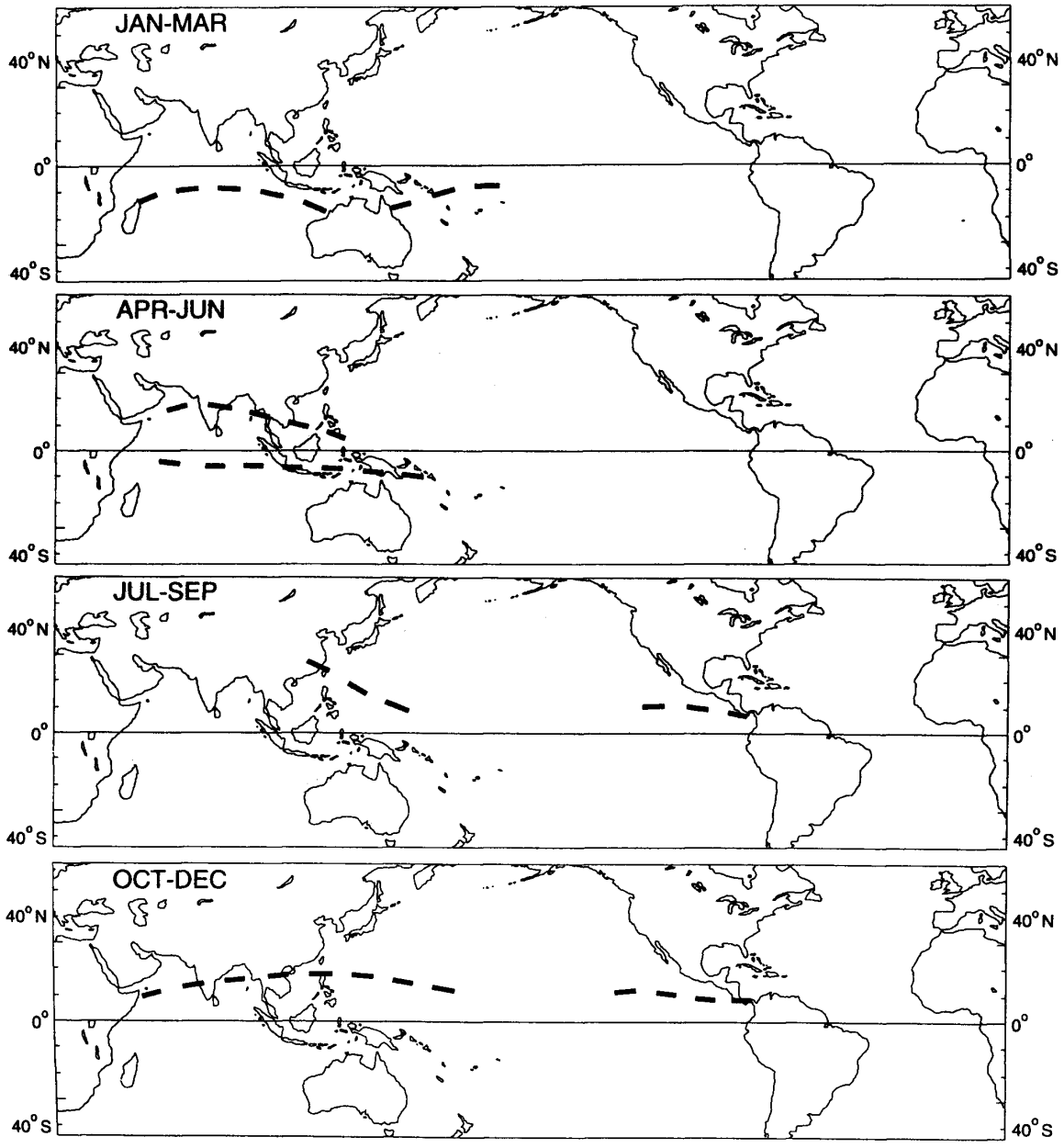

Fig. 3.5 Representative locations of the oceanic monsoon-type ITCZ during various seasons.

The first global climatology of tropical cyclone genesis by Gray (1968, 1975, 1979) demonstrated that the distribution of genesis may be related to six environmental factors:

(i) large values of low-level relative vorticity;
(ii) a location at least a few degrees poleward of the equator, giving a significant value of planetary vorticity;
(iii) weak vertical shear of the horizontal winds;
(iv) sea-surface temperatures (SSTs) exceeding 26°C, and a deep thermocline;
(v) conditional instability through a deep atmospheric layer; and
(vi) large values of relative humidity in the lower and middle troposphere.

The first three factors are functions of the horizontal dynamics, while the last three are thermodynamic parameters. Gray defined the product of (i), (ii,) and (iii) to be the dynamic potential for cyclone development, while the product of (iv), (v,) and (vi) may be considered the thermodynamic potential. The diagnosed tropical cyclone formation frequency (Fig. 3.6a) derived by Gray (1975) using the above parameters is quite similar to the observed formation locations (Fig. 3.6b). However, the combination of the above six parameters were "tuned" to agree with the mean seasonal and geographical distributions of tropical cyclone development. As discussed by Gray (1975) and McBride (1981a), the thermodynamic parameters vary slowly in time and would be expected to remain above any threshold values necessary for tropical cyclone development throughout the cyclone season. On the other hand, the dynamic potential can change dramatically through synoptic activity. Thus, it was hypothesized by Gray that cyclones form only during periods when the dynamic potential is perturbed to a value above its regional climatological mean.

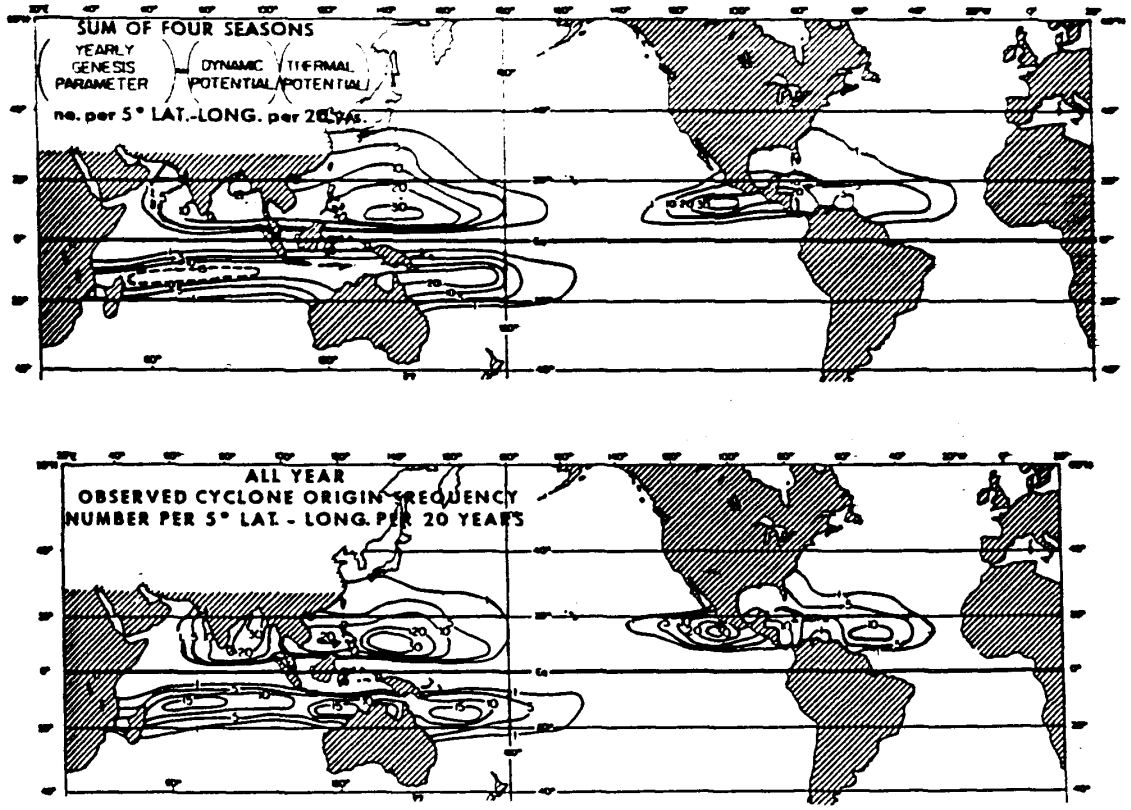

Fig. 3.6 Annual genesis parameter defined by Gray (1975) and (b) observed tropical cyclone formation frequency expressed as occurrence per 20 years within 5° lat.-long. areas.

Frank (1987) noted that the above six environmental parameters are not independent. In the tropics, regions of high sea-surface temperatures are invariably correlated with conditional instability due to the weak horizontal temperature gradients in the lower troposphere. High humidities in the middle levels also tend to occur in convective clusters over warm waters, and virtually all areas with widespread deep convection are associated with mean ascending motion. Thus, Frank reduced the list to four parameters by combining (i) and (ii) into the absolute vorticity at low levels, deleting (v), and adding mean upward vertical motion to (vi). A number of observational studies have derived parameters relevant to the potential of an individual disturbance to develop into a cyclone. These will be discussed in Chapter 3.5.

3.3 REGIONAL CLIMATOLOGIES OF TROPICAL CYCLONE FORMATION

An overview of the climatology of cyclone formation is presented below for each of the tropical cyclone basins. The descriptions are drawn from material presented by participants at the first International Workshop on Tropical Cyclones (IWTC-I), as synthesized by Frank (1987). Differences among the descriptions arise primarily from differences in the observational systems and archived data sets.

3.3.1 North Atlantic

Neumann *et al.* (1993) present the most complete climatology of the Atlantic region, and many other sources are listed in this reference. The annual number of tropical cyclones in this region is highly variable, with totals ranging from 1 to 21 storms during the last century (Fig. 3.7). In addition to high year-to-year variability, a low frequency periodicity is evident between about 1910 and 1930. The data set is not long enough to resolve whether this minimum is part of a statistically significant long-term oscillation. Neumann *et al.* (1993) note that aircraft reconnaissance of cyclones began in this basin during the mid-1940's, so that data from the period 1944-1985 are the most representative of the cyclone frequency in this basin. In addition to the long-term fluctuations in storm frequency, variations occur in the locations of major cyclones (Hebert and Taylor 1983) that are not well understood. Gray (1990) has pointed out that during the 1940's and 1950's large numbers of severe tropical cyclones made landfall along the upper Atlantic coast of the United States. In comparison, fewer than normal such landfalls occurred in the 1970's and 1980's. Gray attributes these differences to the former period being one of abundant rainfall in the Sahel region of Western Africa, while the later period coincided with a two-decade long Sahel drought. According to Landsea and Gray (1992), dry years in the Sahel correspond to increased vertical wind shear over the North Atlantic basin, which thus inhibits cyclone formation. Easterly waves that are spawned in the West African region subsequently become North Atlantic tropical cyclones. Apparently variations in rainfall in the Sahel have an effect on the development potential and subsequent track of the disturbances.

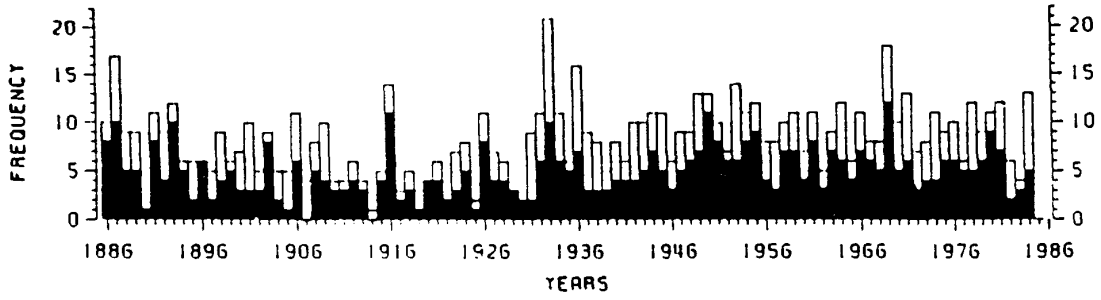

Fig. 3.7 Number of North Atlantic tropical cyclones reaching at least 17.5 m s^{-1} (34 kt) intensity (open bar) and reaching at least 33 m s^{-1} (64 kt) intensity (solid bar) each year during 1886-1985 (provided by C. Neumann).

The North Atlantic is special because it is the only tropical cyclone basin not associated with a monsoon trough, and the seasonal mean flow has a westerly vertical shear (left panel, Fig. 3.4). However, McBride and Zehr (1981) showed that in many instances prior to tropical cyclone formation a shear pattern similar to that of a monsoon trough sets up temporarily in this basin. For example, vertical shear of zonal wind from operational National Hurricane Center analyses (Fig. 3.8) at 60 h prior to the classifications of cyclones Amy and Blanche (1975) as tropical cyclones is similar to the monsoon-type shear pattern in Fig. 3.4.

The seasonal cycle is very pronounced in the Atlantic basin (Fig. 3.9a), with a well-defined maximum in early September and weak (but statistically significant) secondary maxima in June and October. Preferred areas of genesis vary seasonally as well, with more northerly and easterly points of origin in mid-season, when the high sea-surface temperatures and deep easterly flow regions are most extensive.

The modes of genesis of Atlantic tropical cyclone are both well documented and unusual. The origins of each cyclone for each season are documented in annual reports published in the *Monthly Weather Review* (e.g., Pasch and Avila 1992; Mayfield and Lawrence 1991). Slightly more than half of the cyclones form from easterly waves moving westward from Africa. These waves form equatorward of the mid-tropospheric easterly jet at the southern boundary of the Saharan air layer. A small fraction of the storms form along the ITCZ. In this region (and in the western North Pacific), a number also form in subtropical regions near stagnant frontal zones or east of upper-level troughs. These so-called "baroclinic" systems are a special forecast problem in these two basins where the fronts encounter warm waters at relatively poleward locations compared to other basins.

3.3.2 Eastern and Central North Pacific

Because much of the tropical Pacific east of 180° long. is infrequently traversed by ships, the number of tropical cyclones was substantially underestimated before the deployment of weather satellites. An average of 8.6 cyclones was reported between 1949-1964, while the average was 16.5 from 1968-1990. Accepting the latter number as the more accurate estimate, this basin ranks second in annual cyclone frequency (Table 3.1). One of the more interesting aspects is the high concentration of genesis locations in a small region just west of Central America. This area, which has a compact region of sea-surface temperatures above 29°C, has the highest frequency of tropical cyclone genesis per unit area in the world.

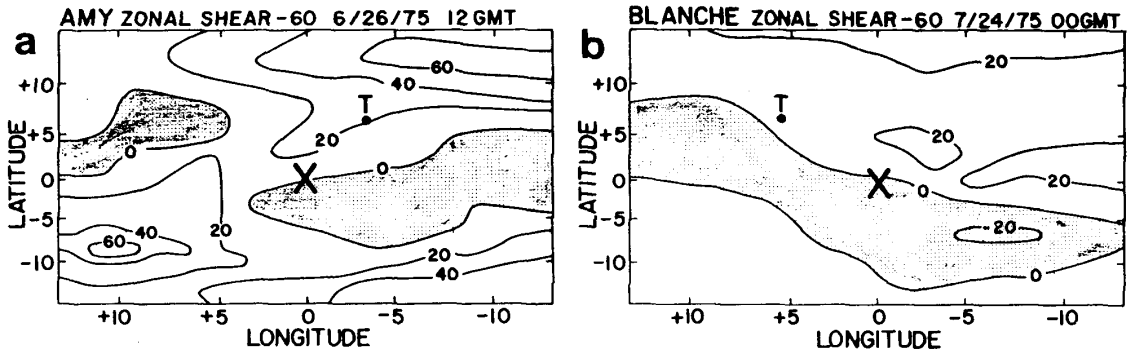

Fig. 3.8 Vertical shear of the zonal wind (kt) between 200 mb and approximately 900 mb for pre-tropical cyclone disturbances in the Atlantic Ocean. Maps are 60 h prior to formation of (a) Amy and (b) Blanche during 1975. Easterly wind shear regions are shaded and storm positions are indicated by crosses at the origin of coordinate system (McBride and Zehr 1981).

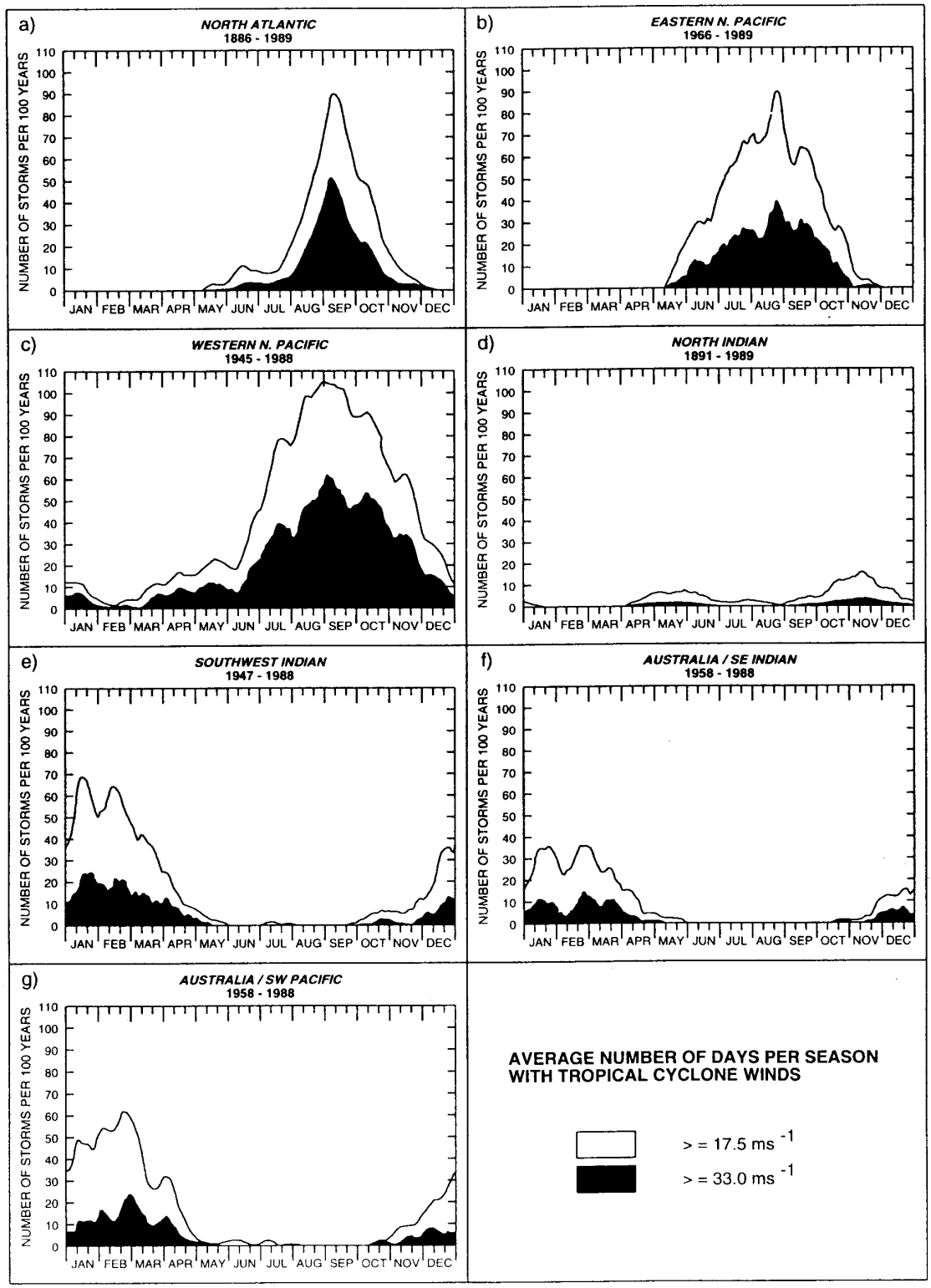

Fig. 3.9 Seasonal tropical cyclone frequency for (a) North Atlantic, (b) eastern North Pacific, (c) western North Pacific, (d) North Indian, (e) Southwest Indian, (f) Australia and Southeast Indian regions, and (g) Australian and Southwest Pacific. Upper and lower bounds refer to maximum winds of at least 34 kt and 64 kt respectively. Data have been smoothed over a 15-day period (Neumann 1993).

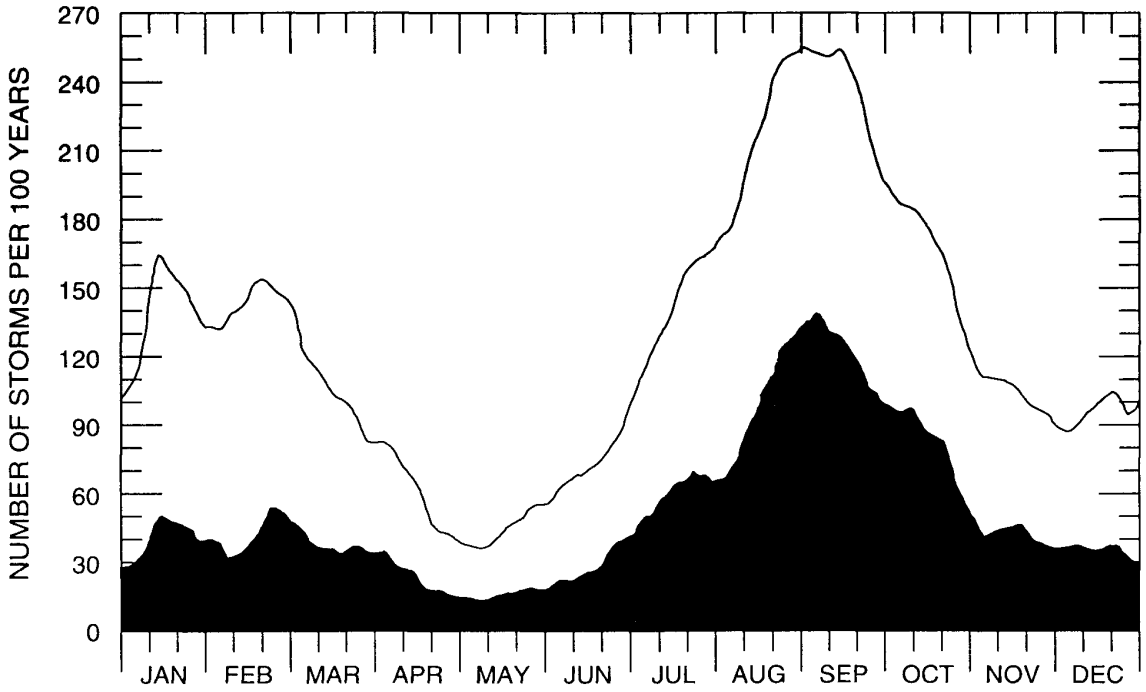

Fig. 3.10 Seasonal tropical cyclone frequency as in Fig. 3.9 except for combination of all basins (Neumann 1993).

The seasonal variation has a single maximum in late August (Fig. 3.9b). The season extends from June to October, which corresponds with the northward shift in the highest water temperatures and in the ITCZ (Allard 1984). Various studies (e.g., Simpson *et al.* 1969; Avila 1991) suggest that many, if not all, cyclone formations in the eastern Pacific region are triggered by Atlantic easterly waves crossing Central America. Neumann (1993) points out that indirect evidence for the hypothesis is found in the seasonal distribution graphs for the North Atlantic and East Pacific basins (Fig. 3.9a, 3.9b). Specifically, relative minima in one basin correspond to relative maxima in the other, and the combined basin profile (not shown) is unimodal.

3.3.3 Western North Pacific

The climatology of the western North Pacific was described by Xue and Neumann (1984). More tropical cyclones form over the western North Pacific than in any other basin, with an average of about 26 each year (Table 3.1). Roughly two-thirds of these become severe tropical cyclones, which are locally known as typhoons. Although highly seasonal (Fig. 3.9c), this is the only region in which tropical cyclogenesis has been observed in all months of the year.

As shown in Fig. 3.1, cyclones occur over a very broad area, although 91% of them originate between 5° and 22°N. As indicated above, preferred regions of formation vary seasonally with the annual migrations of the maximum sea-surface temperatures and the ITCZ. The western North Pacific is particularly noted for the occurrence of very large and very intense tropical cyclones. The most obvious reason for the large numbers is the extremely large area of very warm water, with some regions having temperatures exceeding 30°C from July-October. During the summer, the warm waters of the western North Pacific lie just to the west of the Tropical Upper Tropospheric Trough (TUTT) and near the entrance of the upper tropospheric tropical easterly jet that lies over the Indian Ocean. Both of these features may contribute to broad regions of upper-level divergence, which is thought to be favorable for cyclone genesis. Sadler (1978) has described the role of the TUTT in the genesis of tropical cyclones.

Tropical cyclones in this area are well documented in a series of annual reports published by the United States Joint Typhoon Warning Center (JTWC) at Guam. The initial disturbances most frequently (about 80%) form in the monsoon trough, and the remainder form from waves in the easterlies (perhaps 10%), in conjunction with upper cold lows, or in the baroclinic zones of intruding midlatitude troughs. A particularly dangerous type of development occurs about once per year in the East China Sea when a wave in the easterlies overtakes a surface depression and leads to rapid formation of typhoons within 24 h of landfall on the coast of China.

3.3.4 North Indian Ocean

Although only about 7% of the global tropical cyclones occur in the North Indian Ocean (Table 3.1), they are the most deadly. The shallow waters of the Bay of Bengal, the low flat coastal terrain, and the funnelling shape of the coastline can lead to devastating losses of life and property due to the surge from a storm of even moderate intensity. The Buckerganj cyclone of 1876 and the Bhola cyclone of 1970 each killed more than 200,000 persons in Bangladesh. As recently as 1991, more than 100,000 people were killed by a storm surge in Bangladesh.

About five to six cyclones form in this basin each year, with variations from one to 10 during the period 1890-1989. Since these cyclones form from an average of 16 disturbances, about 35% of the initial disturbances reach tropical cyclone strength, and 45% of these cyclones reach the severe tropical cyclone stage. About five to six times more tropical cyclones occur in the Bay of Bengal as in the Arabian Sea (Fig. 3.11). Although large variability in the locations of storms from decade to decade has been reported, no systematic patterns have been determined.

The seasonal variation has a bimodal distribution with the primary maximum in November and a secondary maximum in May (Fig. 3.9d). That is, the intervening period of the summer monsoon is a relatively suppressed period of tropical cyclone formation. McBride (1986) attributed this suppression to the close interrelation between tropical cyclones and monsoon depressions. The two types of systems have almost identical structure of the larger scale vortex, and both systems form over warm tropical oceans. During the May and June cyclone season, systems develop this large-scale vortex structure in the monsoon trough and remain over the ocean long enough to develop an inner core structure, and so become tropical cyclones. When the monsoon trough is located farther north and closer to land in August, the systems still form over warm waters, but they then track northwest onto the Indian subcontinent and so remain monsoon depressions (i.e., with no inner-core structure). Similar inter-relationships between monsoon depressions and tropical cyclones have been documented for the two Australian cyclone basins by McBride and Keenan (1982) and Davidson and Holland (1987).

Although the development from a tropical depression into a tropical cyclone usually occurs in about 12-24 h, 15% require more than 48 h and others are reported to undergo formation in less than 12 h (Srinivasan and Ramanamurty 1973). Most North Indian Ocean cyclones form within the monsoon trough. Formation may occur either as reintensification of westward-propagating disturbances or from *in situ* disturbances that develop within the trough. The zone of formation shifts meridionally between 5° - 20°N following the annual migration of the monsoon trough.

3.3.5 Southwest Indian Ocean

As shown in Fig. 3.9e, the major part of the cyclone season extends from November through March, with a double peaked mid-season maximum (in mid-January and mid-February.) The morphology of formation is quite poorly documented in this basin due to the sparsity of synoptic and upper-air data. The mean position of the 26°C SST isotherm is generally south of 20°S during the peak of the season, and retreats equatorward to about 5-10°S during the winter.

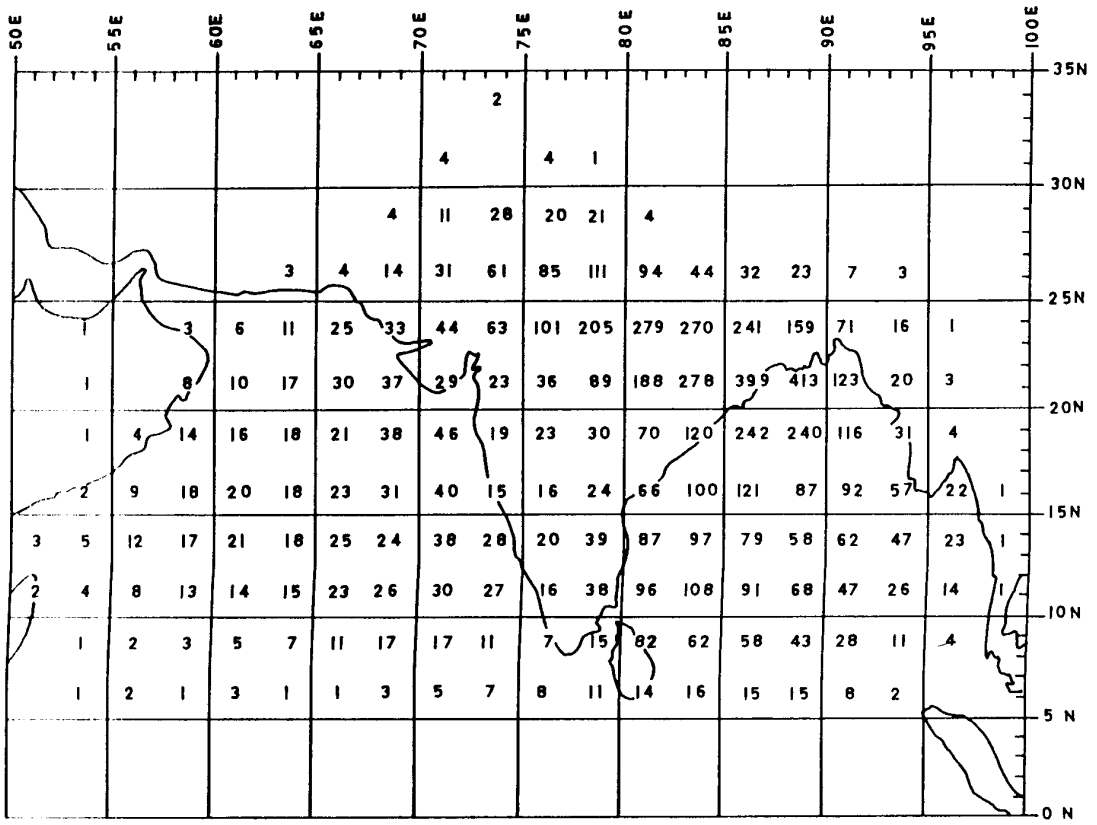

Fig. 3.11 Number of tropical cyclones passing through each 2.5 deg. lat.-long. box during January-December 1877-1974 (Mandal and Neumann 1976).

The seasonal establishment and retreat of the Southern Hemisphere monsoon shearline are consistent with the seasonal variation of cyclone formation. In particular, the shearline is at its farthest excursion from the equator during January and February and the formation locations follow a similar trend (Fig. 3.12). However, the far western portion of this basin (between the African coast and 50°E) has a different behavior. No formations occur in this region until November. Most of the formation events that do take place in this area are confined to the Mozambique Channel between the African mainland and Madagascar, which leads to a marked poleward displacement of these initial positions relative to the positions over the ocean east of 50°E. A distinct transition in the surface wind flow through the Mozambique Channel occurs between November and December with a change from the dominant southeasterly trade regime of November to a cross-hemispheric northerly flow in December. This northerly component remains a prominent feature of the general circulation through February, but the flow retreats equatorward during March. By April, the general flow reverses as the southeasterly trade winds become dominant and tropical cyclone activity ceases in the area.

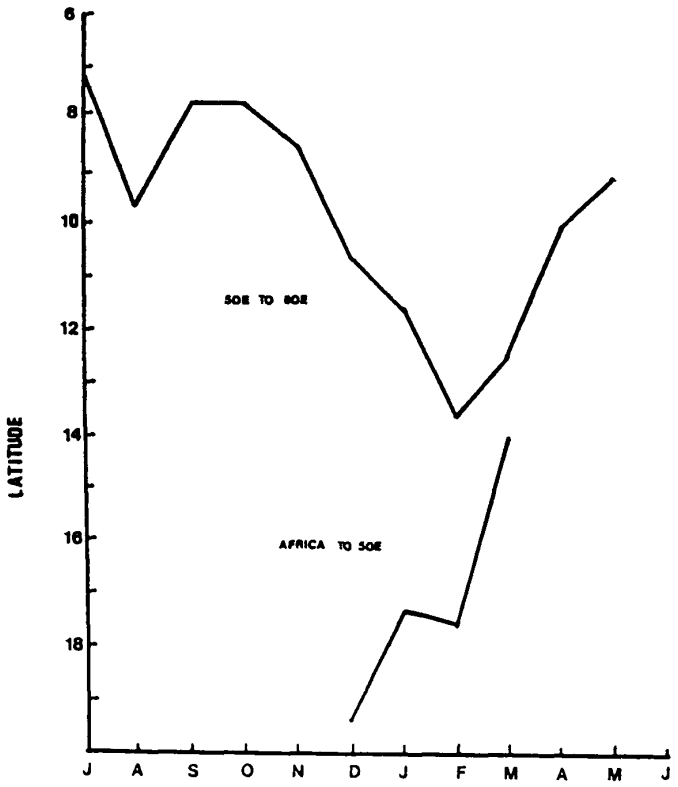

Fig. 3.12 Mean monthly latitudes of initial pre-tropical cyclone disturbances that later had intensities of at least 34 kt in the Southwestern Indian Ocean. Upper curve is for 50°E - 80°E and lower curve is for region from African coast to 50°E (provided by G. Foley).

3.3.6 Southeast Indian Ocean/Australian basin and Southwest Pacific/Australia basin

The frequency of occurrence of tropical cyclones in these two basins is mapped in Fig. 3.13. Notice the proximity of cyclone formation to the Australian continent. Based on a 20-year climatology of formations between 105° and 165°E, McBride and Keenan (1982) found approximately 50% of the formation points (i.e., classification as a tropical cyclone) occurred within 300 km of land. Three major centers of tropical cyclone occurrence are: (i) off the Northwest coast; (ii) in the Gulf of Carpentaria; and (iii) in the Coral Sea. A minimum in activity just eastward of Cape York Peninsula near 145°E is attributed by Holland (1984c) to the effects of the continent on the large-scale thermal and moisture fields. He notes that the highest frequency of systems attaining only tropical cyclone status is in the landlocked Gulf of Carpentaria, with secondary maxima in the Coral Sea and off the Northwest coast. By comparison, severe tropical cyclones have a very high frequency off the Northwest Australian coast, occur only occasionally in the Gulf of Carpentaria, and are spread more widely throughout the Southwest Pacific.

As discussed by McBride and Keenan (1982) and Holland (1984a, b, c), the vast majority of cyclones in these basins form from disturbances in the monsoon trough. A relative minimum in activity occurs in the Southeast Indian Ocean/Australian basin (i.e., west of 142°E) during the mid-season (Fig. 3.9f), when the monsoon trough is located over land. The latitudes of origin exhibit a strong seasonal cycle with early- and late-season cyclones forming closer to the equator than mid-season. It is noteworthy that approximately half of the cyclones that form off the northwest Australian coast are from initial "pre-cyclone" disturbances that form over the Australian continent.

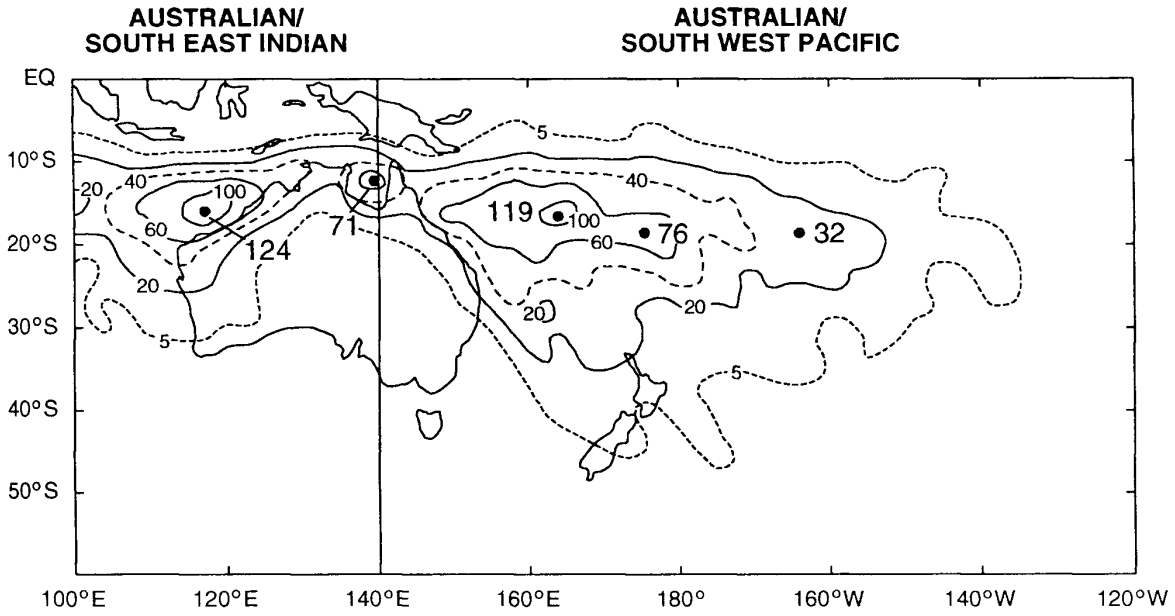

Fig. 3.13 Frequency of tropical cyclones per 100 years passing within 75 n mi (139 km) from given points in the Australia/South Indian Ocean region (adapted from Neumann 1993). Circles indicate relative maxima.

In the eastern portion of the Southwest Pacific basin, the monsoon trough merges with the South Pacific Convergence Zone (SPCZ). In this region, formation of a tropical cyclone pair occurs approximately two or three times per year (Keen 1982; Lander 1990). Each member of the pair is at approximately the same latitude and longitude, but on opposite sides of the equator. Both members of the pair reach severe tropical cyclone status about once every two or three years. The low centers of the two symmetric circulations about the equator produce strong westerly winds along the equator called westerly wind bursts. Ramage (1986) and Keen (1982) have hypothesized these cyclone pairs and their associated westerly wind bursts influence the evolution of the planetary scale Southern Oscillation in subsequent months.

3.4 INTERANNUAL VARIATIONS OF TROPICAL CYCLONE ACTIVITY

3.4.1 Predictability and seasonal forecasts

As indicated in the rows along the bottom of Table 3.1, most cyclone basins have relatively large interannual variabilities in cyclone activity. The ratio of the standard deviation in cyclone numbers to the mean ranges from 25 to 40%, while the corresponding ratio for severe tropical cyclones ranges from 34 to 69%. The exception is the western North Pacific basin, which has a (relatively) small variability with a ratio of only 16% for cyclone numbers and 23% for severe tropical cyclone numbers.

A number of authors have demonstrated relationships between the interannual fluctuations in cyclone numbers and slowly varying aspects of the large-scale tropical circulation. The significance of the term "slowly varying" is that such relationships may then be used to forecast tropical cyclone activity in advance by monitoring the large-scale atmospheric (and oceanic) structure at the beginning of the cyclone season.

The pioneering work in this field was by Nicholls (1979, 1984, 1985) for cyclones in the two Australian basins. He demonstrated an association between the Southern Oscillation Index (SOI) during the Southern Hemisphere winter and the number of tropical cyclones close to Australia (from 105° - 165°E) during the subsequent cyclone season (i.e., from October to April). The number of cyclone days over a season is correlated with mean sea-level pressure for the preceding July-September (Fig. 3.14). The linear correlation coefficient for the two series over this 25-year sample is -0.68. Nicholls (1985)

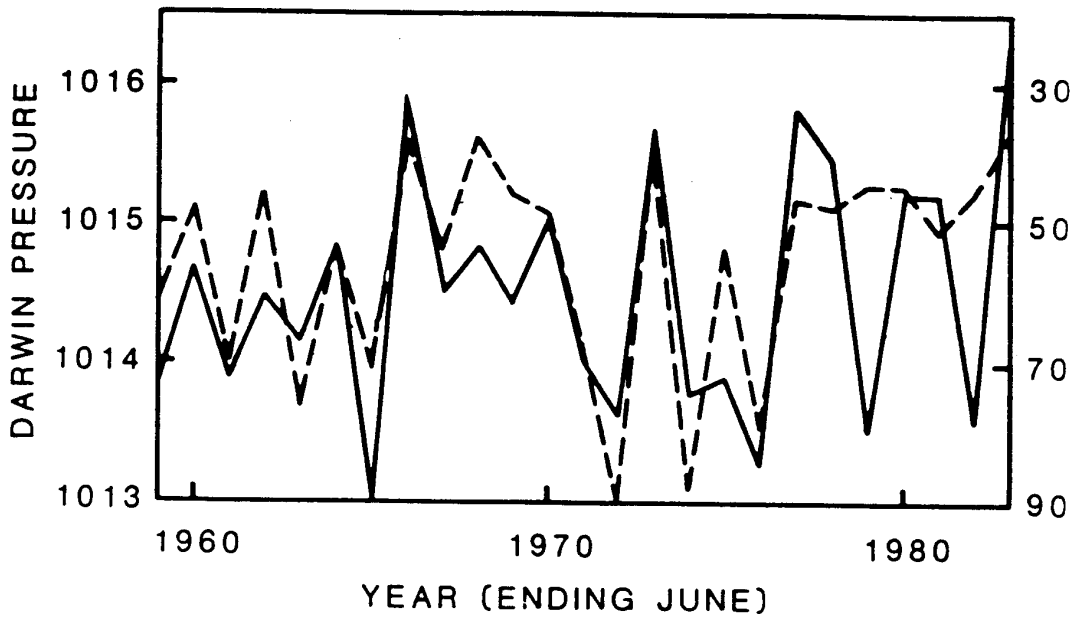

Fig. 3.14 Time series of number of cyclone days in the Australian region (105°-165°E) during the 1958/59 - 1982/83 cyclone seasons (dashed line, right scale reversed) and mean Darwin 0900 UTC mean sea-level pressure for July-September prior to the cyclone season (solid line)(Nicholls 1985).

demonstrated the robustness of the relationship by calculating separate lag correlations for each ten-year data set from 1909 to 1982. For all seven 10-year subsets, the correlation coefficient between July-September pressure and subsequent October-April cyclone numbers ranged from -0.41 to -0.72 (provided he removed one "bad" data point for the 1943/44 cyclone season).

However, Nicholls (1992) detected a sudden decrease in cyclone numbers within the region following the end of the 1985/86 season that has not been accompanied by a corresponding decrease in the Southern Oscillation Index (SOI). Thus, his method would have consistently over-predicted cyclone activity during the 1986/87 - 1990/91 seasons. This sudden change in the SOI-cyclone numbers relationship may have been a real physical change, or is perhaps a result of changes in satellite imagery interpretation, or inadvertent changes in the Southern Oscillation Index. Nicholls (1992) suggests that a possible remedy may be to correlate the trend in the SOI versus the change in cyclone numbers from one season to the next.

The second major work on seasonal prediction of tropical cyclone activity has been for the North Atlantic basin. Relationships between numbers of cyclones and the large-scale pressure patterns were originally found by Namias (1955) and Ballenzweig (1959). Major developments in documenting the predictability of this basin have been recently achieved (Gray 1984a, 1984b, 1990; Gray *et al.* 1992, 1993; Shapiro 1982a, 1982b, 1987, 1989). The number of tropical cyclones in a season has been related to various aspects of the large-scale flow, including the sea-level pressure, the patterns of sea-surface temperature, the upper-tropospheric zonal winds, and seasonal rainfall in the Sahel of West Africa. The strongest relationships have been with the Southern Oscillation and with the stratospheric Quasi-Biennial Oscillation (QBO), which is a quasi-periodic reversal of zonal winds over the Equator. The tropical cyclone activity in seasons during the west phase of the QBO is a factor of 1.4 greater than during the east phase. Ascribing a simple index of +1 for a season in the west phase, 0 for transition seasons and -1 for east phase of the QBO, the correlation of this index with the cyclone numbers accounts for 33% of the variance. Similarly, large correlations are found between cyclone numbers and an index of Southern Oscillation/El Nino activity based on SST anomalies over the equatorial eastern Pacific.

Using an algorithm based on the lagged relationships between cyclone numbers and the above indices of the large-scale circulation, Gray has issued public forecasts during May each year from 1984 through 1993 for measures of Atlantic cyclone activity in the following season. Mean values, mean errors, and correlation coefficients between Gray's forecasts and measures of actual cyclone activity are given in Table 3.2. The highest correlation coefficient for this sample of ten seasons is the forecast of the number of tropical cyclones. A time series of actual versus forecast value of the number of tropical cyclones is shown in Fig. 3.15.

Some limited potential for seasonal prediction has been found in the western North Pacific. Zhang *et al.* (1990) studied interannual variations of cyclones in this basin during the peak months of July - October for 1959 - 1979. They found that 40% of the variance in this series could be explained through regression with the SOI and the trend in the SOI series. However, no significant trend for this basin can be detected in the numbers in Table 3.1. Inspection of Zhang *et al.*'s data reveals their observed trend is heavily

Table 3.2 Forecast statistics for four indices of tropical cyclone activity for the North Atlantic basin as forecast by W. Gray during May preceding the ten seasons from 1984 to 1993. An intense hurricane refers to Saffir-Simpson categories 3, 4, or 5.

Indices	Observed Mean	Mean absolute error	corr. coef.
No. of cyclones	9.5	1.8	0.59
No. of intense hurricanes	5.1	1.4	0.42
No. cyclone days	43.31	1.8	0.26
No. intense hurricane days	17.1	9.4	0.33

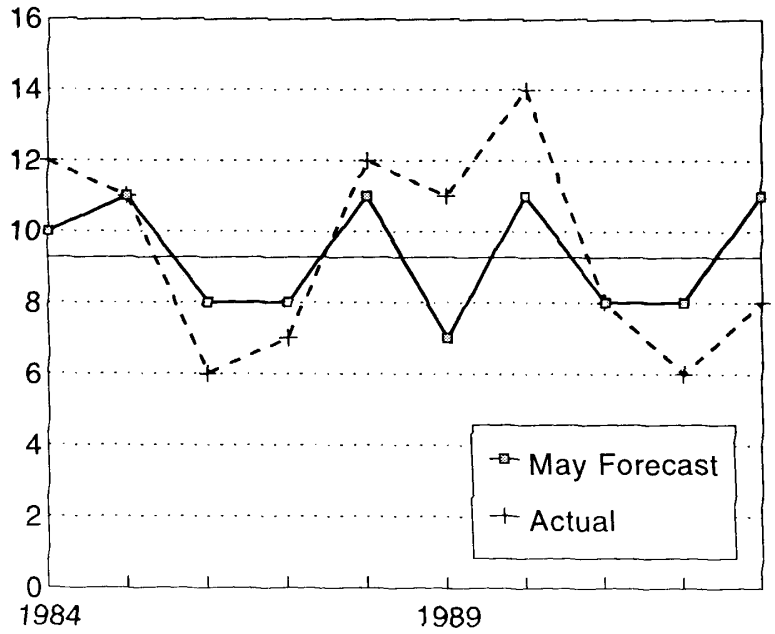

Fig. 3.15 Forecast (solid) versus observed (dashed) number of tropical cyclones in the North Atlantic basin for 1984 to 1993. The forecasts are those issued to the public by W. Gray during May preceding the cyclone season each year, and may be compared with the long-term mean frequency (thin).

influenced by large values in the first nine years of their series (i. e., the years prior to the beginning of the data in Table 3.1). Thus, any firm conclusions on predictability of annual tropical cyclone occurrence for this basin must await analysis with a longer time series.

3.4.2 Associations with the Southern Oscillation

Each of the above three forecast relationships for annual tropical cyclone activity included some aspect of El Nino/Southern Oscillation (ENSO) phenomenon as a key component. Nicholls' forecasts for the Australian region are based completely on various indices of the Southern Oscillation. The correlation of cyclone numbers in the Australian region and the SOI in the months preceding the season is approximately 0.7 (i.e., accounting for 50% of the variance). Perhaps the physical reason for the association is that the number of tropical cyclones during the season has a simultaneous high negative correlation with the large-scale surface pressure in the region; i.e., a low surface pressure is consistent with a large number of tropical cyclones. Since northern Australia is close to one of the centers of action of the Southern Oscillation, variations in this large-scale pressure are effectively equivalent to variations in the SOI. The predictability (or lag relationship) comes through the slow variation (or large serial correlation) of the SOI at the time of year preceding the Southern Hemisphere cyclone season.

During an ENSO warm event in eastern Pacific, the pressure over Australia is high, which leads to a reduced number of cyclones in that region. Revell and Goulter (1986a, b), Hastings (1990), and Evans and Allen (1992) have pointed out that the frequency of cyclone formation at the eastern end of the Australian/South Pacific basin (i.e., east of 170°E) actually increases during an ENSO warm event. Although the relationship between the formation longitudes in the region and the SOI is weak, it is statistically significant. However, the relationship appears to be dominated by the extreme events (i.e., warm events). If the relationship is real, the eastward movement of formation locations may be explained in terms of the favorable factors for cyclone formation discussed in Chapter 3.2. During an ENSO warm event, the region with SSTs exceeding 26°C extends much farther eastward across the South Pacific. Of probably more importance, the Southern Hemisphere monsoon westerlies extend to the dateline, which means that the monsoon shearline extends much farther eastward.

A number of authors have studied the association between the SOI and cyclone activity in the western North Pacific basin (Chan 1985; Dong 1988; Zhang et al. 1990; Lander 1994). In each study, the simultaneous SOI relationship with the total number of cyclones over the basin has been quite weak. However, Chan (1985) reports that the number of cyclones east of 150°E increases when the large-scale pressure is high, i.e., during an ENSO warm event. The reason (given by Chan) is the same as given above for the South Pacific. During an ENSO warm event, the monsoon shearline extends farther eastward than normal, which is a condition conducive for cyclone formation. This was extended by Lander (1994) who showed that a large number of monsoon-shearline type cyclone formations occur late in the season of a warm event in a region east of 160°E and south of 20°N. Conversely during a cold event, no formations occur in that southern and eastward part of the basin.

The relationship between ENSO and cyclone activity in the North Atlantic basin apparently is quite different. Shapiro (1987) reports a correlation of -0.34 (only 12% of the variance) between cyclone numbers and the warm water anomaly in the equatorial eastern Pacific. Both Shapiro (1987) and Gray (1984a) give evidence that the physical link is that higher equatorial SST values increase the activity of tropical convection, which increases the upper-level westerly zonal winds and the vertical wind shear downstream over the primary formation region of the Atlantic cyclones. As discussed above, large vertical shear represents an unfavorable condition for tropical cyclone formation (on this seasonal timescale).

Table 3.3 Linear correlation coefficients between the series of tropical cyclone numbers in Table 3.1 and the Troup Index of the Southern Oscillation (anomalies of monthly Tahiti minus Darwin sea-level pressure differences normalized by the standard deviation of the Tahiti minus Darwin series). The upper row is for the entire 22-year series and the second row is for the series omitting the extreme values (upper and lower) of the SOI series. For the four Northern Hemisphere basins, the SOI has been averaged from July to September, while it is averaged over January to March for the three Southern Hemisphere basins.

Correlation coefficient	North Atlantic	Eastern North Pacific	Western North Pacific	North Indian	Southwest Indian	Australia/ SE Indian	Australia/ SW Pacific
22 year series	+0.31	+0.00	+0.13	-0.04	+0.19	+0.37	-0.01
20 year series	+0.29	+0.20	+0.35	-0.17	+0.07	+0.19	+0.01

For completeness, the time series of tropical cyclones in each basin listed in Table 3.1 have been correlated with the simultaneous SOI (Table 3.3). Positive correlations are calculated for four of the seven basins with the 22-year series. Although the largest values are for the Australian/Southeast Indian basin and for the North Atlantic, the percentage of explained variance is small (14% and 10%, respectively). Inspection of the SOI time series for January-March showed that the 1982-83 El Nino value was well outside the range of values for the remainder of the series, which may have an undue influence on linear correlations. To test the robustness of the correlations, the years with the extreme positive and the extreme negative SOI values were excluded from the time series and the correlation analysis repeated. The large change in correlation coefficients between the 22-year series and the 20-year series (Table 3.3) indicates some caution is necessary in inferring physical relationships based on this short of a time series.

Using consistency between the two rows of Table 3.3 as a criterion for robustness, three basins appear to have consistent correlations between cyclone numbers and the SOI: Australian/Southeast Indian, North Atlantic, and western North Pacific. During an ENSO warm event, when the pressure is high at Darwin, the number of cyclones is suppressed near Australia and in the North Atlantic. For most climatic parameters, the relationship with the SOI has the opposite sign in the West Pacific from the West Atlantic. The reason for the consistent sign with tropical cyclones is because of the two very distinct physical mechanisms explaining the relationships, as has been described above.

Longitudinal displacements in the formation areas are not revealed in Table 3.3 because of the basin boundary definitions. In particular, Nicholls indicates a correlation coefficient of approximately 0.7 between the SOI and the combined number of tropical cyclones in the Australian/Southeast Indian basin and the western end of the Australian/Southwest Pacific basin. Although a smaller positive correlation is calculated for the Australian/Southeast Indian (Table 3.3), a zero correlation is found for the entire Australia/Southwest Pacific basin, which is sufficiently large that a decrease in cyclone numbers at the eastern end of the basin (following Nicholls) offsets an increase in cyclone numbers at the western end (following Revell-Goulter) during an ENSO warm event.

3.4.3 Associations with sea-surface temperature

Following Palmen (1948), it has been generally accepted that tropical cyclones only form when the underlying SST exceeds 26°C. Statistically significant relationships have not been demonstrated for any basin between cyclone numbers and simultaneous values of SST. This is consistent with Palmen's hypothesis that the temperature criterion is one of

threshold rather than proportionality. Zhang *et al.* (1990) found quite high correlations between cyclone numbers in the western North Pacific and higher latitude SSTs (i.e., north of the typical formation locations). Shapiro (1982b) found positive correlations between North Atlantic cyclone activity and SSTs immediately west of Africa (i.e., in the source region of the easterly waves).

An interesting association between cyclone occurrence and SST occurs in the oceans surrounding Australia. As discussed above, cyclone frequency in this region is significantly correlated with the SOI, which is in turn related to the SST values north of Australia. The SSTs at the beginning of the season correlates at approximately 0.8 with the seasonal total number of cyclones (Nicholls 1984). In the middle of the season, the SST-cyclone number correlation is close to zero, and the SST at the end of the season correlates with the seasonal number of cyclones at approximately -0.4. A cause-and-effect in the sense that the cyclone activity is responsible for the decrease in large-scale SST has not been established. This should be amenable to investigation given the recent availability of real-time analyses of SST.

In a more comprehensive study, Raper (1992) correlated tropical cyclone numbers for seven cyclone basins with the three-monthly average SST near the beginning of the season (May-July for Northern Hemisphere basins and either September-November or October-December for Southern Hemisphere basins) for the period 1900-1986. Time series of the 15-year running mean correlation coefficients for each basin are shown in Fig. 3.16. The SSTs are averaged over the sub-portion of the basin with the highest correlation coefficients with the total cyclone numbers for that season. Positive correlations that remain consistent throughout the record are found only for the Atlantic, the Australian region and (possibly) the eastern North Pacific. None of these basin correlations imply a strong *in situ* relationship. The area of high correlation for the North Atlantic is the same area found by Shapiro (1982b), i.e., near Africa, which is to the north and east of the location of cyclone formation. For the eastern North Pacific, the highest correlation of the SST subdomains is near 20°N, north of both the cyclogenesis region and the main cyclone tracks. For the Australian region, Raper's findings duplicate those of Nicholls described above, and thus hold only for SST *at the beginning of the season*. Thus as stated by Raper, *"the separation between the regions of SST influence and the storms themselves argues that these positive correlations are not a direct result of higher SSTs being more favorable for tropical cyclone formation and intensification. Rather, the cause for the link appears to be the atmospheric conditions to which both the SSTs and the tropical cyclone frequencies are intimately related."*

3.4.4 Final comments on interannual variations

Demonstration of the potential for prediction of tropical cyclone activity based on data available at the beginning of the season is one of the major breakthroughs in the field of tropical cyclone formation. The two strongest large-scale signals are the Southern Oscillation (Chapter 3.4.2) and the stratospheric QBO. A statistically significant relationship with the QBO has been established only for the Atlantic basin, and a physical link between the stratospheric zonal winds and tropical cyclone formation has not been demonstrated.

Relationships between cyclone numbers and both the QBO and the SOI may have important implications for the effects of future climate changes on tropical cyclone numbers. A valid climatic prediction technique of expected cyclone numbers would require a reasonable prediction of how the climatic changes will affect the large-scale controlling influences, and also assumes that the present associations with cyclone numbers will continue to hold. Given the lack of any strong relationship between cyclone numbers and simultaneous SSTs, we are not currently in the position to make any predictions concerning changes in the frequency of tropical cyclone formation associated with climate changes that may be induced by increasing concentrations of greenhouse gases.

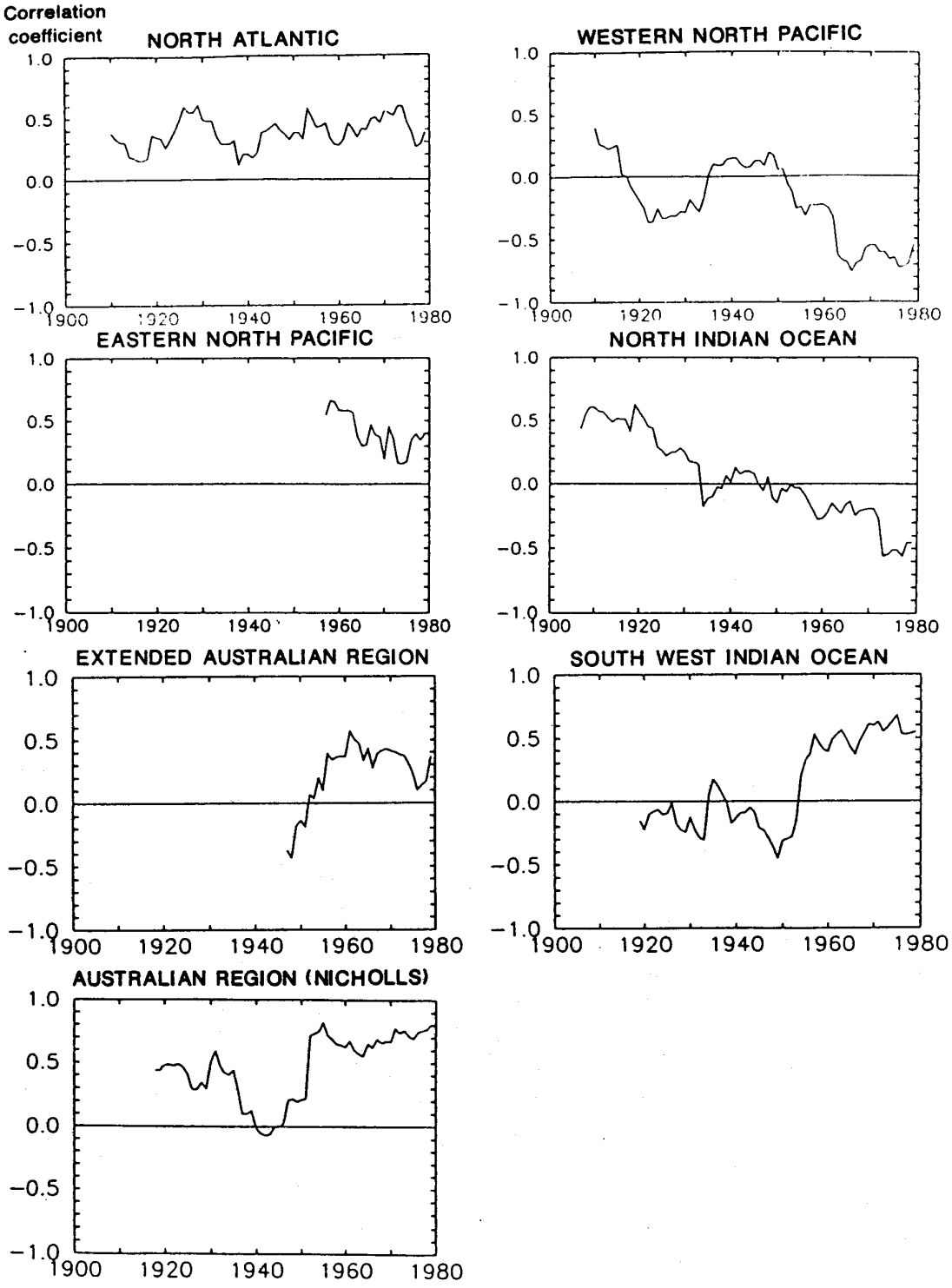

Fig. 3.16 Correlation coefficients (15-y running mean) between tropical cyclone frequencies and three-month average SSTs for each cyclone basin, where these SSTs are averages over the sub-portion of the basin with the largest correlation coefficient with total cyclone numbers (Raper 1992).

3.5 LARGE-SCALE CONDITIONS ASSOCIATED WITH TROPICAL CYCLONE FORMATION

Tropical cyclones form only over the tropical oceans where upper-air observations are sparse, which has made it difficult to document the structure and evolution of the flow during the formation process. Consequently, much of the early understanding of formation was gained from case studies based on innovative use of the existing data networks (e.g., Riehl 1948; Hubert 1955; and Yanai 1961). Subsequent studies that exploited improved observational systems have led to further refinement and detail in documentation of the tropical cyclone formation process. However, no well-accepted, closed theory of formation exists (as will be discussed in Chapter 3.6).

The observational studies have isolated a number of synoptic-scale aspects that have an important role in the formation process:

(i) Tropical cyclones form from pre-existing disturbances containing abundant deep convection;
(ii) The pre-existing disturbance must acquire a warm core thermal structure throughout the troposphere;
(iii) Formation is preceded by an increase (spin-up) of lower tropospheric relative vorticity over a horizontal scale of approximately 1000 to 2000 km;
(iv) A necessary condition for cyclone formation is a large-scale environment with small vertical shear of the horizontal wind;
(v) An early indicator that cyclone formation has begun is the appearance of curved banding features of the deep convection in the incipient disturbance;
(vi) The inner core of the cyclone may originate as a mid-level meso-vortex that has formed in association with a pre-existing mesoscale area of altostratus (i.e., a Mesoscale Convective System or MCS); and
(vii) Formation often occurs in conjunction with an interaction between the incipient disturbance and an upper-tropospheric trough.

Evidence for these seven observations will be described in the following subsections.

3.5.1 Pre-existing disturbance

"We observe universally that tropical storms form only within pre-existing disturbances ... An initial disturbance therefore forms part of the starting mechanism. A weak circulation, low pressure, and a deep moist layer are present at the beginning. The forecaster need not look into areas which contain no such circulations." These statements by Riehl (1954) have stood the test of time. The key characteristic defining a pre-cyclone disturbance is a persistent region of cumulonimbus convection (and associated altostratus decks) that extends over several hundred kilometers. Examples of pre-cyclone disturbances for the western North Pacific basin are shown in Fig. 3.17. The structure of these tropical "cloud clusters" has been documented by many authors (e.g., Ruprecht and Gray 1976a,b; Johnson and Houze 1987). The cloud clusters have an upper-tropospheric warm core and mean (averaged over a 4 deg. lat.-long. square) upward velocities of about 100 mb/day (McBride and Gray 1980; Lee 1989). Although the diameter of the convective area is typically only a few hundred km, the rotational circulations associated with the systems usually extend over a diameter of approximately 1000 - 1500 km. For example, North Atlantic cloud clusters are frequently associated with wave troughs in the easterlies. As discussed in Chapters 3.3 and 3.4, a close association between tropical cyclone formation and the monsoon trough exists on seasonal and climatological time scales. However, not all pre-existing disturbances are in the monsoon trough. For instance, 16 % of pre-cyclone disturbances in the Australian region are not associated with the trough (McBride and Keenan 1982), and 35% in the western North Pacific are not associated with the trough (Zehr 1992).

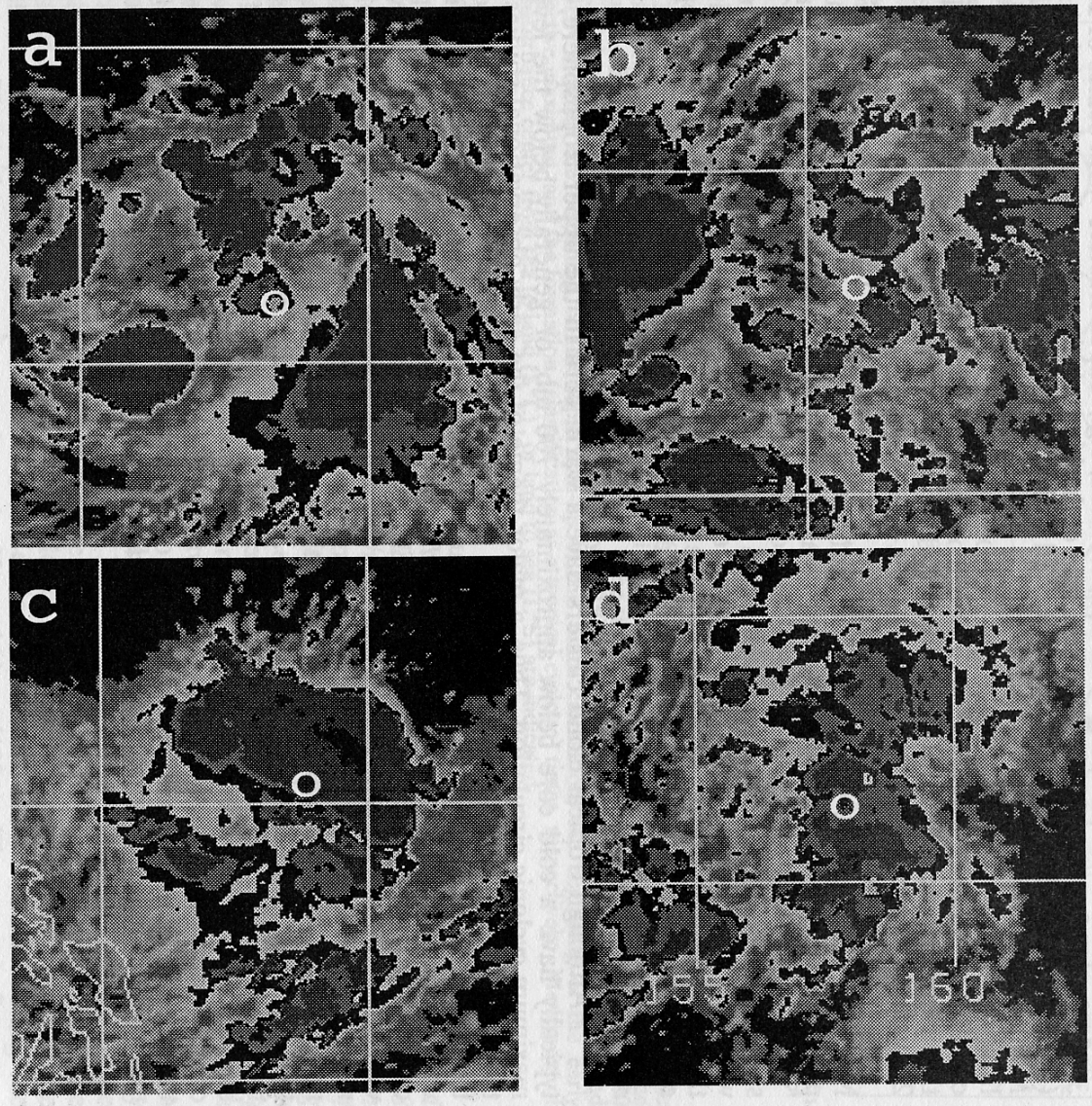

Fig. 3.17 Enhanced satellite images showing the pre-cyclone disturbance 48 h prior to classification as a tropical cyclone for four cyclones occurring in the western North Pacific: (a) Irving 00 UTC 31 July 1992; (b) Janis 18 UTC 1 Aug 1992; (c) Lois 00 UTC 15 Aug 1992; and (d) Robyn 06 UTC 31 July 1993. The enhancement is such that the inner-most black areas are temperatures lower than -80°C, and the adjacent dark gray, gray, and then black regions represent temperature increases in 5°C intervals. A standard gray scale is used for temperatures between -65°C and -30°C, and temperatures higher than -30°C are set to black. The background grid squares are 5° lat. by 5° long. (which corresponds to about 555 km at these latitudes). The approximate center is indicated by the white circle (provided by M. Boothe, Naval Postgraduate School).

An important condition is that the pre-cyclone cloud cluster must be "persistent." A forecaster rule-of-thumb in many basins is that any cloud cluster that persists for several days has a high probability of becoming a tropical cyclone. For the western North Pacific formation region during July-December 1983 and 1984, Zehr (1992) found only 22 non-developing cloud clusters that persisted for more than two days, whereas about 50 tropical cyclones formed. That is, a persistent cloud cluster had approximately a 70% probability of becoming a tropical cyclone.

The period of time between first detection of the pre-cyclone cloud cluster and formation (i.e., classification as a tropical cyclone) is highly variable. McBride and Keenan (1982) found that the pre-cyclone disturbance stage east of Australia lasted approximately 1 - 2 days. For cyclones forming to the north or west of Australia, this stage was typically about 2 - 4 days, with occasional pre-cyclone periods of up to 10 days. Zehr (1992) found the period between the "early convective maximum" and formation in the western North Pacific averaged 3.2 days, but it ranged from less than 1 day to more than 8 days.

Over the western North and South Pacific tropics, the cloud cluster convection is often embedded within a larger scale circulation, e.g., "super-clusters" with scales of 2000 - 3000 km. These super-clusters are in turn embedded within eastward-moving global scale (5,000 to 10,000 km) circulations associated with the 30-60 day oscillations (Lau *et al.* 1991; Manton and McBride 1992). Frank (1987) hypothesized that tropical cyclone formation is linked to these 30-60 day oscillations in tropical surface pressures, upper-level winds, and cloudiness. Frank's hypothesis followed from an earlier observation by Gray (1979, 1985) that global tropical cyclone formations tend to occur in clusters of 2-3 weeks separated by 2-3 weeks of inactivity.

Liebmann *et al.* (1994) confirmed the relationship for both the Southern and Northern Hemisphere portions of the Indian Ocean and the western Pacific Ocean. In particular, they found approximately twice as many tropical cyclone formations occur in the "wet" (low pressure) phase of 30-60 day oscillation as occur in the "dry" phase. They showed this relationship is entirely due to a greater number of depressions occurring in the wet phase of the oscillation. Once the depression (or initial disturbance) has formed, it has the same probability of developing further into a tropical cyclone or a severe tropical cyclone, independent of the phase of the oscillation.

3.5.2 Lower-tropospheric warm core

Although tropical cloud clusters have a warm core in the upper troposphere, they typically have a cold core below approximately 700 mb, or generally below the level of maximum cyclonic circulation. Thus, a major theme of the early observational studies was the mechanism for transformation from a cold core to a warm core in the lower troposphere (Riehl 1948; Hubert 1955; Yanai 1961). A transformation from cold core to warm core was observed by Davidson *et al.* (1990) prior to the formation of two tropical cyclones during the Australian Monsoon Experiment (AMEX). These two cyclones were well observed as they formed within an approximately 600 km diameter array of six rawinsonde stations. The relative vorticity of the pre-cyclone disturbances (Fig. 3.18) has a maximum at approximately 700 mb during the early stages, which implies a cold core below that level by thermal wind considerations. Approximately 2 - 3 days prior to cyclone formation, the vorticity maximum migrates downward to approximately the top of the boundary layer (900 mb), which implies the establishment of a lower-tropospheric warm core. The physical mechanism for this downward migration of the mid-level vortex toward the surface, and thus into contact with the oceanic heat and moisture source, is one of the missing links in our understanding of tropical cyclone formation.

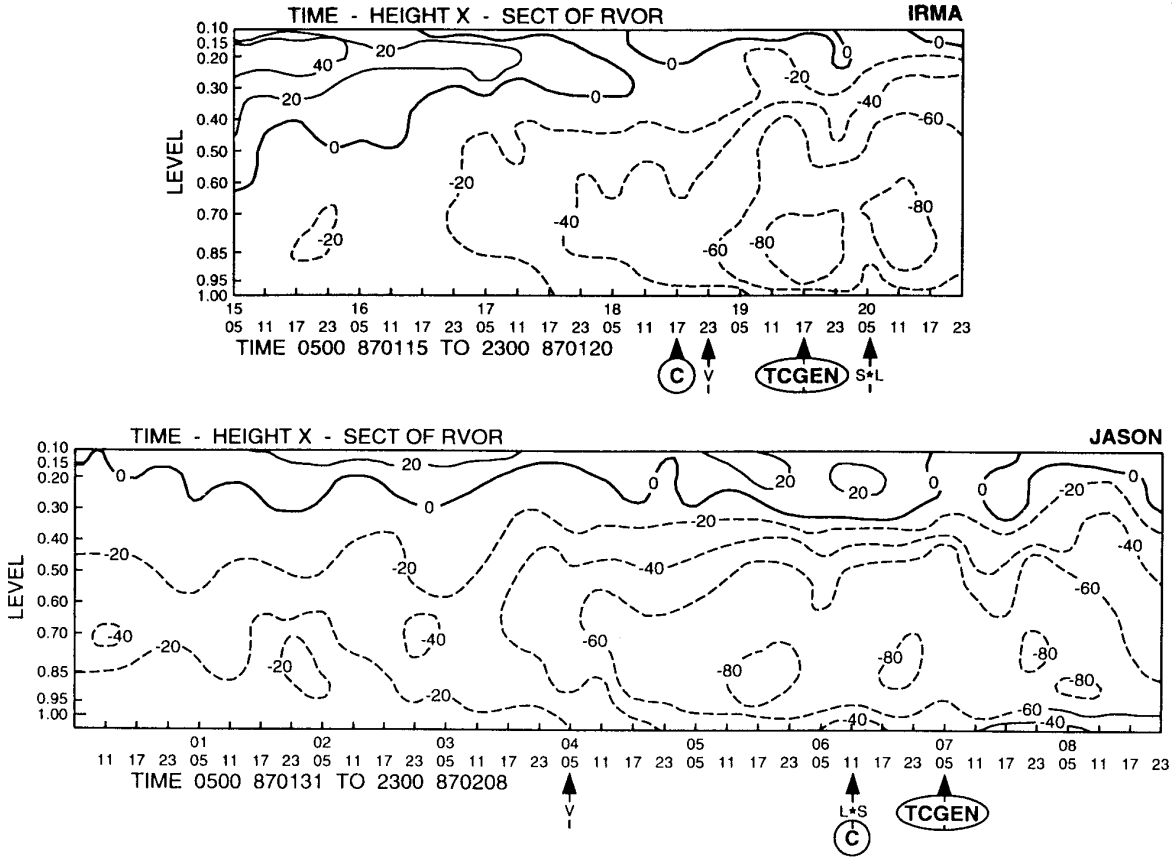

Fig. 3.18 Time-height sections of relative vorticity (10^{-6} s^{-1}, cyclonic is negative) over a 300 km radius circle surrounding the disturbance that developed into tropical cyclones Irma (upper) and Jason (lower) during the Australian Monsoon Experiment (Davidson *et al.* 1990). The time axis is from 0500 UTC 15 January to 2300 UTC 20 January 1987 (upper) and 0500 UTC 31 January to 2300 UTC 8 February (lower). Labels V, C, and TCGEN indicate the beginning of the rapid spin-up of this outer circulation, the beginning of the early convective maximum, and the formation (classification as a tropical cyclone) times, respectively. Movement of the disturbance center from sea to land (S*L) , or land to sea (L*S) are indicated.

3.5.3 Large-scale spin-up

McBride and Zehr (1981) concluded that *"The developing or pre-typhoon cloud cluster exists in a warmer atmosphere over a large horizontal scale, for example, out to 8 degrees latitude radius in all directions ... Pre-typhoon and pre-hurricane systems are located in large areas of high values of low-level relative vorticity. The low-level vorticity in the vicinity of a developing cloud cluster is approximately twice as large as observed with non-developing cloud clusters."* Thus, one of the first stages of the process of tropical cyclone formation is this spin-up of the large-scale envelope. This spin-up in the two AMEX cyclones (Fig. 3.18) is revealed by an increase in the relative vorticity over the 300 km radius circle from approximately 20 (10^{-6}) s^{-1} to approximately 40 (10^{-6}) s^{-1} several days prior to formation.

In some cases, the large-scale spin-up is due to an enhancement of the flow on either side of the monsoon trough. The westerlies on the equatorial side of the ITCZ may increase due to cold surges from the winter hemisphere, which raises pressures at the equator and subsequently leads to stronger pressure gradients and westerly flow along the equator as in Fig. 3.19 (Love 1985a,b). Examples of interactions between long waves in the Southern Hemisphere and equatorial westerlies in the western North Pacific during the Northern Hemisphere summer were shown by He and Yang (1981). The easterly flow on

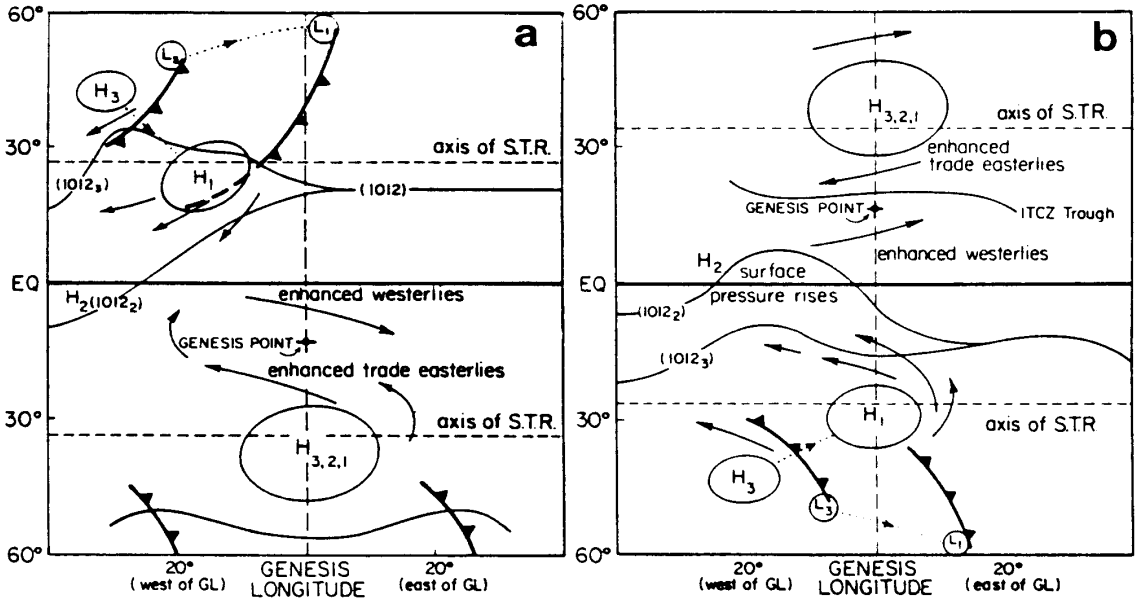

Fig. 3.19 Schematic surface map of the positions of important synoptic-scale features 3 days and 1 day before cyclone genesis in (a) Southern and (b) Northern Hemisphere. Subscripts on the highs (H) and lows (L) denote days before genesis (Love 1982).

the poleward side of the monsoon trough also may increase as a result of intensification of the subtropical ridge. Tropical cyclones seldom form until this zonally-oriented ridge moves sufficiently poleward to establish strong, deep trade easterlies. The strength of the trades along the equatorward side of the subtropical ridge has long been used as a potential indicator for tropical cyclogenesis in the western North and South Pacific (e.g., Chen and Ding 1979).

Davidson and Hendon (1989) presented evidence that the large-scale spin-up preceding formation occurs as a downstream development mechanism associated with energy dispersion of low-latitude Rossby waves. Their analysis was for Southern Hemisphere cyclone developments during the Winter Monsoon Experiment (MONEX) during 1978-79. Davidson *et al.* (1990) substantiated the Davidson and Hendon mechanism also occurred during the AMEX season (1986-87), and McBride *et al.* (1995) demonstrated that it occurred during TOGA-COARE (1992-93).

Several authors have recently proposed that an *in-situ* spin-up of the ITCZ or monsoon trough may occur when two or more pre-existing regions of high potential vorticity (PV) values interact, rotate around each other, and eventually merge into one large region of enhanced PV. Based on this idea, two complementary mechanisms have been proposed. Guinn and Schubert (1993) proposed that an elongated PV zone representing the ITCZ may form into separate vortices due to barotropic instability of the mean flow (see Fig. 3.27). Ritchie *et al.* (1993) focused on mesoscale vortices that are assumed to be generated within the mesoscale altostratus decks in cloud clusters in the monsoon trough. Certain configurations of these mesoscale regions of enhanced PV, or certain configurations of large-scale flow, are hypothesized that lead to a merger into one large rotation center that represents an enhanced monsoon trough vortex.

Another factor that may significantly alter the likelihood of cyclone genesis is the presence of a nearby mature cyclone. Frank (1982) showed that tropical cyclones affect the circulation pattern within 1000-2000 km of the storm center in such a way as to enhance the

potential for formation of another storm in the wake and to inhibit formation ahead of the storm. The primary mechanism is through modulation of the large-scale vertical velocity fields, because ascent is favored in the wake and subsidence ahead of the center.

3.5.4 Small vertical wind shear

As discussed in Chapter 3.2, one of the environmental factors associated with the mean seasonal and geographical distributions of tropical cyclone frequency is small vertical shear of the horizontal wind. For example, Gray (1984a) and Shapiro (1987) have found inverse relationships between cyclone numbers in the North Atlantic and seasonal mean vertical shear (Chapter 3.4.2). It is also generally accepted that a small vertical wind shear is a necessary condition for an individual pre-existing disturbance to develop into a tropical cyclone. This condition is listed in virtually all forecaster handbooks and in reviews of the subject (e.g., Palmén 1956; Atkinson 1971; Bureau of Meteorology 1978; Riehl 1979; Anthes 1982; Frank 1987). The physical reason usually given for the importance of small (or even zero) shear is to accumulate moisture and temperature anomalies in a vertical column above the incipient disturbance. By contrast, the presence of large vertical shear is said to "ventilate" the column by advecting the warm core aloft away from the low-level circulation center. Some support for this idea is provided in the numerical simulations of Tuleya and Kurihara (1981), Kurihara and Kawase (1985), and Tuleya (1988). In those studies, the vertical shear had to be such that a strong vertical coupling exists via the phase speed of the incipient (low-level) disturbance and the upper-level winds. This coupling serves to keep the warm area above the disturbance and thereby maintains a favorable condition for growth of the disturbance.

Despite this consensus, little evidence exists on a case-by case basis that a simple index such as the magnitude of the vertical shear is a discriminating factor between developing and non-developing disturbances. For the western North Pacific basin, Zehr (1992) compared the vertical shear in 22 persistent non-developing cloud clusters with that of the 50 pre-cyclone clusters. He found virtually no difference, with the pre-cyclone clusters having a mean shear (200 - 850 mb) of 10.1 m s^{-1} and a standard deviation of 5.3 m s^{-1}, whereas the values for the non-developing clusters are 10.2 and 5.1 m s^{-1}, respectively. Because Zehr only included cloud clusters that persisted at least two days, vertical shear below some threshold value may be a necessary condition for the existence of such persistent, organized convection.

In their radiosonde composite study, McBride and Zehr (1981) found the pre-cyclone systems had zero vertical shear directly over the center, but very large vertical shears equatorward in the equatorial westerlies and poleward in the trades. For example, large westerly shear (greater than 20 m s^{-1}) is found poleward of the precursor disturbances to Amy and Blanche with easterly shear equatorward (Fig. 3.8). To quote from their paper, *"this result helps clear up some of the confusion that has existed in the past concerning vertical wind shear and tropical cyclogenesis. There has been some resistance, for example, to acceptance of low tropospheric vertical shear as a cyclogenesis requirement. This hesitation has stemmed partly from synoptic observations of strong shears close to the developing systems. Forecast schemes based on low shear will give a high score to a tropical area of low shear. Such schemes work well on a climatological basis, but for individual situations ... there is actually a requirement not only for very small vertical shear near the system center but also for two adjoining regions of strong 200-900 hPa vertical shear of opposite sign on either side of the system."*

One of the most widely used techniques for the operational analysis and forecasting of tropical cyclone formation is satellite imagery interpretation data following the methods of Dvorak (1975, 1984). According to that technique, cyclone formation is greatly inhibited when the cloud patterns indicate strong upper-level flow in a uniform direction. Although this is often referred to as development being *"inhibited by strong vertical shear,"* it is strong *"uni-directional shear"* that seems to be unfavorable.

3.5.5 Curved cloud features

Although the horizontal scale of the pre-existing convective cloud cluster is usually of the order of 500 km, it may range from as small as 200 km to as large as 1500 km. A persistent cloud cluster consists of many Mesoscale Convective Systems (MCSs) that are continually evolving on time scales of 6-18 h. These MCSs are associated with a number of cumulonimbus elements that feed moisture to a deep altostratus deck (which are shown as "white" regions in Fig. 3.17).

Dvorak (1975, 1984) states that the convective elements form into curved cloud lines or bands approximately 36 h prior to classification as a tropical cyclone. According to Dvorak, *"a T1 classification is made when curved cloud lines or bands indicate that a system center has been near to or within a deep-layer convective cloud system for a period of at least 12 hours.....It is the close association of moderately curved cloud lines or bands and a sizable amount of deep-layer convection that signals cyclogenesis."* This configuration can appear in various forms (Fig. 3.20).

Zehr (1992) documented several satellite-observed characteristics of pre-cyclone disturbances in the western North Pacific. A very large diurnal variation of convection and altostratus occurs with a maximum around 0600 local time. The overall trend of convection (24 h running mean) attains a maximum near the time of maximum intensity increase (i.e., during the *intensification* phase as distinct from the *formation* phase). Nevertheless, a convective maximum is associated with the pre-tropical cyclone disturbance even before it is classified as a tropical depression. In Zehr's sample, the convective maximum occurs in 80% of pre-cyclone disturbances. It typically precedes by three days classification as a cyclone, with a range between 15 h and 8 days. Similar phenomena have been observed by Steranka *et al.* (1986) and Davidson *et al.* (1990), both of whom noted that the convective maximum coincides with a weakening of the diurnal signal. Appearance of the early convective maximum prior to the two AMEX cyclones in Fig. 3.18 is marked by the letter "C" along the time scale. In the conceptual model by Zehr (1992) of tropical cyclone formation (Fig. 3.21), the early convective maximum is indicated during stage one. Other aspects of this diagram will be discussed in Chapter 3.5.6.

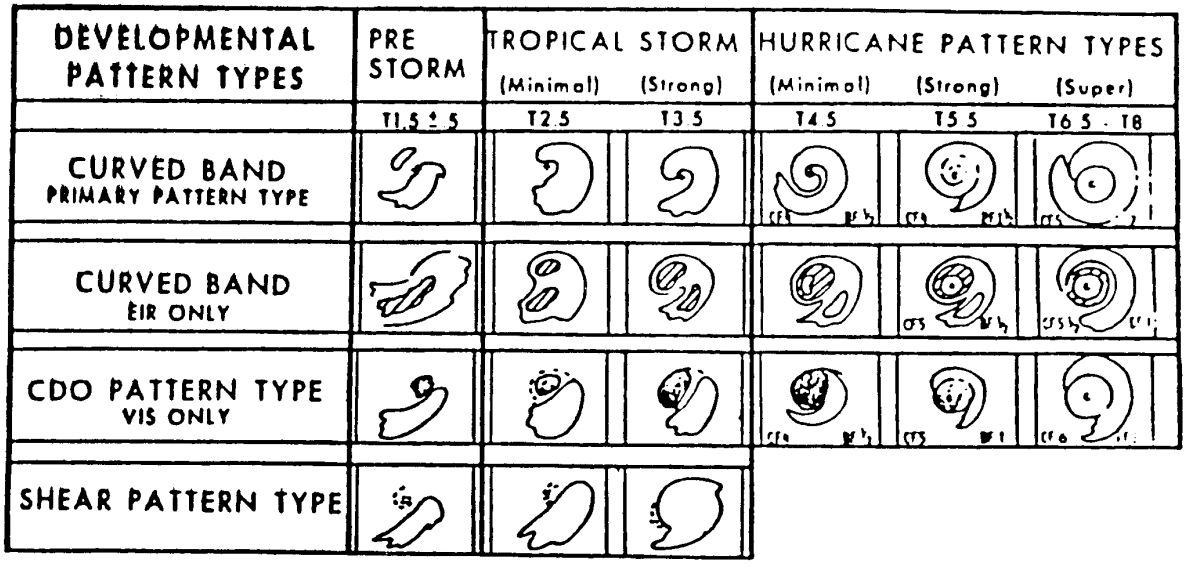

Fig. 3.20 Cloud pattern types in the tropical cyclone intensity analysis based on satellite imagery. Pattern changes from left to right are typical 24-hourly changes (Dvorak 1984).

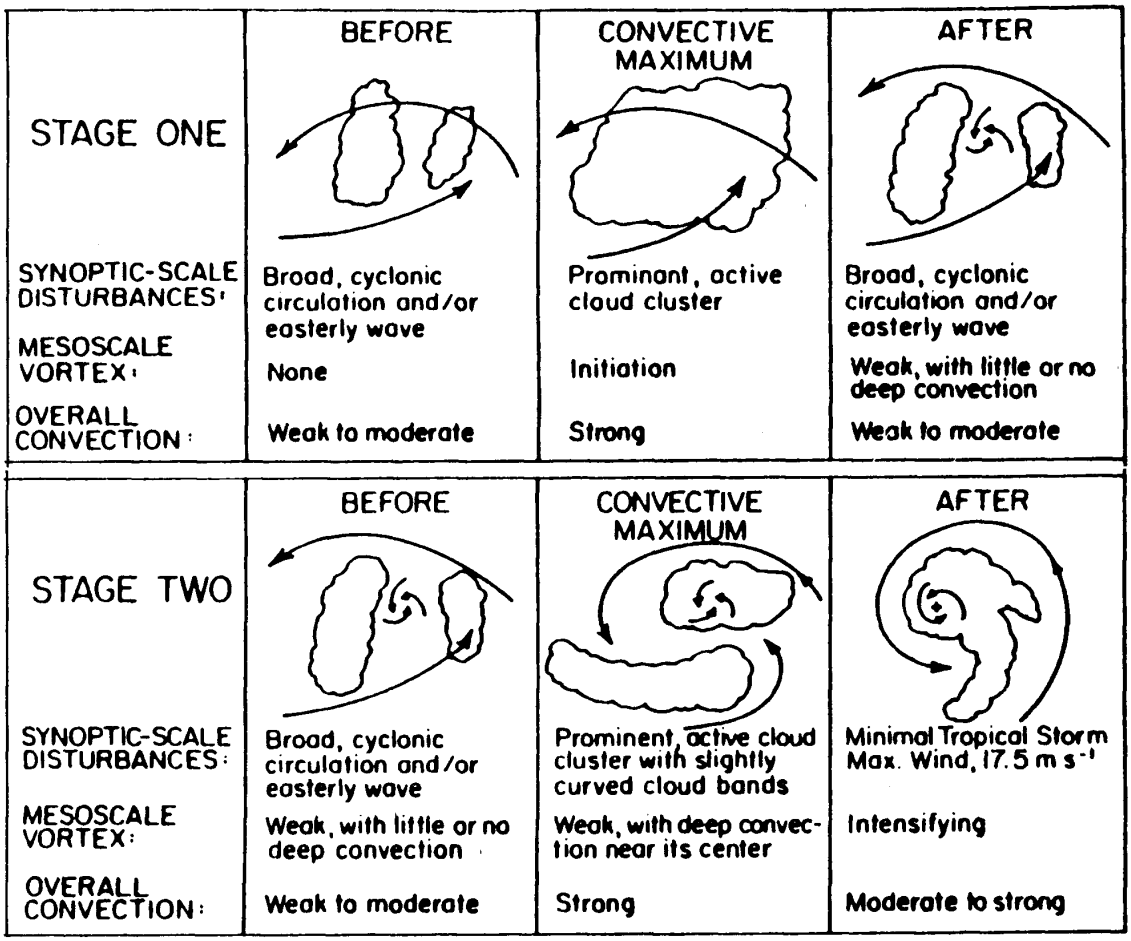

Fig. 3.21 Conceptual model of two stages in tropical cyclone formation based on case studies with visual and infrared satellite images in the western North Pacific (Zehr 1992).

3.5.6 Mid-level mesoscale vortex

Mesoscale Convective Complexes (MCC's) were first identified as long-lived convective weather systems in the middle latitudes by Maddox (1980), Fritsch and Maddox (1981), and Bosart and Sanders (1981). Similar systems have been identified in other regions of the world (Houze *et al.* 1981; Velasco and Fritsch 1987; Miller and Fritsch 1991). The defining conditions for MCCs involve threshold values in the enhanced IR imagery that are appropriate for midlatitude systems. Since lower threshold temperatures are appropriate in the tropics, the more generic term Mesoscale Convective System (MCS) will generally be used here. In the examples of pre-cyclone cloud clusters in Fig. 3.17, the MCSs can be identified as the large areas of cloud with temperatures lower than -70°C, which signifies the presence of long-lived altostratus decks. A pre-cyclone cloud cluster may contain one or more MCSs.

Studies (e.g., Leary and Rappaport 1987; Brandes 1990) over the data-rich area over the United States have indicated that some MCS develop an inertially stable, warm-core vortex in a trailing stratiform region that is referred to as a Mesoscale Convective Vortex (MCV) (Chen and Frank 1993). These MCVs often become evident in visible satellite imagery during later stages of the cycle. In midlatitude MCCs with an intensifying MCV,

the system becomes stronger, persists longer, and induces heavy precipitation (Bosart and Sanders 1981; Kuo *et al.* 1986). In some cases, the vortex appears to be responsible for subsequent development of MCCs (Menard and Fritsch 1989).

Velasco and Fritsch (1987), Frank and Chen (1991), and Chen and Frank (1993) have hypothesized that *"if an MCC forms or propagates into a large-scale environment favorable for tropical cyclogenesis, the MCC-generated warm-core vortex may play a catalytic and crucial role in initiating tropical storm development"* (Velasco and Fritsch 1987). Such a hypothesis appears to be consistent with the study of Zehr (1992) based on satellite data, operationally analyzed wind fields, and reconnaissance aircraft data in the western North Pacific. Recent aircraft-based field experiments called TCM-92 in the western North Pacific (Dunnavan *et al.* 1993; McKinley and Elsberry 1993) and TEXMEX in the eastern North Pacific (Emanuel 1993; Emanuel *et al.* 1993; Lopez *et al.* 1993) have established that MCVs do form in the altostratus decks of tropical MCSs. When it forms, the mesovortex has a horizontal scale of approximately 100 to 200 km. In the early stages, the vorticity maximum is in the middle troposphere between 700 and 300 mb and no appreciable vorticity is detected near the surface. In the TEXMEX studies, the surface flow is divergent below the mesovortex. McKinley and Elsberry (1993) and Ritchie (1993) note that the pre-cyclone cloud cluster may contain a number of "secondary" mesovortices that appear to be directly related to altostratus areas associated with strong convection.

These preliminary observations suggest that the central core of the cyclone may begin as a small vortex at middle levels that extends downward toward the surface and increases in horizontal scale. For consistency with the observational studies discussed in Chapter 3.5.1 - 3.5.3, this mesovortex must exist within a rotational convergent envelope on a larger scale (i.e., the 1000 km outer vortex scale).

Zehr (1992, 1993) and Emanuel (1993) have divided the formation process into two or more stages with an important transition point being the formation of the persistent mesoscale vortex. In Zehr's stage 1 (Fig. 3.21), a mesocale vortex is embedded within the pre-existing disturbance (cloud cluster) circulation. During stage 2, the central pressure of that vortex decreases and the tangential wind increases to result in a minimal tropical cyclone.

3.5.7 Interaction with upper-level disturbances

Case studies by many authors (Riehl 1948; Bath *et al.* 1956; McRae 1956; Fett 1966, 1968; Ramage 1974; Sadler 1976, 1978; McBride and Keenan 1982; McBride and Holland 1989) have demonstrated an apparent initiation of the formation process through interaction with surrounding upper-tropospheric synoptic systems, particularly upper-level troughs. In particular, Sadler (1976, 1978) showed that cyclone formation in the western North Pacific frequently occurs in association with intense cyclonic cells embedded within a large-scale climatological feature known as the Tropical Upper Tropospheric Trough (see Fig. 2.19). McBride and Keenan (1982) showed that rapidly developing tropical cyclones in the Australian region were associated with slowly moving troughs in the upper troposphere displaced by approximately 15 deg. long. on either side of the developing disturbance. On the other hand, slowly developing cyclones were associated with fast moving upper-level troughs, which usually lay over the disturbance at the time of classification as a tropical cyclone.

Bath *et al.*, McRae, and Sadler hypothesized that the upper-level troughs played a kinematic role in that the associated divergence patterns facilitated the development of the tropical cyclone's characteristic upper-level outflow channel. However, McBride (1981b) and Holland (1983) demonstrated that developing tropical cyclones are characterized by large imports of relative angular momentum by eddy fluxes at outer radii in the upper troposphere. Thus, the role of the adjacent upper-level troughs is to provide a flow geometry that brings about this eddy import of angular momentum. Additional observational support for this role for developing monsoon depressions is given by

Davidson and Holland (1987) and for the formation of the two AMEX tropical cyclones by Davidson *et al.* (1990). As discussed in Chapter 2.4.1, observational and modelling studies have demonstrated that upper-level troughs can have a similar role during the intensification stage.

3.6 THEORETICAL MODELS AND PHYSICAL CONCEPTS

No primary mechanism has been isolated as being responsible for the formation of tropical cyclones. It is generally accepted that the basic source of energy for the formation of a tropical cyclone is the latent heat released in clouds, and that in turn is acquired from the underlying sea through the surface evaporative flux E_o. As shown in Chapter 2, the *mature* tropical cyclone is a vertically stacked, warm-core vortex occupying the complete depth of the troposphere. The tangential winds are to first order in gradient balance with this warm core. Frank (1987) noted that the average rainfall within the inner 200 km radius of a typhoon averages about 10 cm/day^{-1}, which provides sufficient latent heat release to heat the atmosphere from the surface to 100 hPa at a rate of about 25°C/day^{-1}. Although rainfall in a cloud cluster is approximately 1/4 this value, it is still sufficient to heat the troposphere by 6°C/day^{-1}. In a *non-developing* cluster, this latent heat release is offset by the expansion cooling in the ascending cores, and the net warming is small (order of tenths of a degree). When a tropical cyclone actually forms, the net response is of the order of 1°C day^{-1} warming integrated through the depth of the troposphere.

The approximate balance in the tropics between the diabatic heating and the adiabatic cooling associated with upward vertical motion can be understood in terms of scaling of the large-scale equations (e.g., Charney 1963; Webster 1983), or in terms of geostrophic adjustment theory, or of Eliassen balanced vortex theory (e.g., Chapter 5 of Charney 1973b). In summary, the ambient conditions in the tropics are such that inertial effects dominate over rotational effects. Consequently, the energy released as heat is distributed in the form of potential energy over very large areas by gravity waves and by slowly varying divergent or secondary circulations. For this reason, theoretical studies of tropical cyclone formation have addressed processes that would allow the cloud cluster to retain the heat release locally.

Another fundamental question to the understanding of tropical cyclone formation is that of scale selection. Theoretical models of convection in a *saturated* environment have maximum growth at vanishingly small horizontal scales, i.e., the scale of individual cumulus clouds. A conceptual breakthrough occurred in the early 1960's in a series of studies that modelled tropical cyclone formation due to the Conditional Instability of the Second Kind (CISK) mechanism (Charney and Eliassen 1964; Ooyama 1964; Ogura 1964; Kuo 1965; Syono and Yamasaki 1966). The CISK mechanism does require that the atmosphere be conditionally unstable (lapse rate between dry and moist adiabatic rates), but does not require large-scale saturation. In the presence of a background rotational field, the effect of the heating on the large-scale flow assumes a different functional form. Specifically, the cloud-scale condensation rate is proportional to vertical motion along a moist adiabat. In contrast, the collective effects of the heating on the large-scale motions are due to a distribution of individual cumulonimbus and mesoscale updrafts, downdrafts, altocumulus anvils, cloud radiative effects, etc.

A third issue in understanding the dynamical reasons for tropical cyclone formation is that it is a multi-stage process. Following the terminology of Chapter 3.5, these stages include the large-scale spin-up, the formation of the pre-existing convective disturbance or cloud cluster, the formation of a persistent mesoscale vortex, and the formation of an eye. It is highly likely that different dynamical mechanisms may be responsible for these different stages of formation. Once a particular stage of formation (even the first) has been reached, the other stages may follow automatically given the presence of sufficiently high sea-surface temperatures and given no dramatic changes in the large-scale flow.

Another consideration is the simulation of tropical cyclone formation in numerical weather prediction models, which are run routinely over the global tropics by a number of

forecast centers. These models achieve some level of success in producing vortices in approximately the same location and time that a tropical cyclone forms in the atmosphere (Fiorino *et al.* 1993; McBride *et al.* 1993). In addition, numerous successful simulations of tropical cyclone formation have been achieved in research-oriented versions of numerical weather prediction models (Davidson and Kumar 1990; Puri and Miller 1990; Tuleya 1988, 1994; Krishnamurti *et al.* 1994), which may imply that the same dynamical processes are responsible in both systems. Accordingly, these simulations may provide a data set for the understanding of tropical cyclone development. However, not all stages of cyclone formation have been simulated in these models. In particular, the development of a mesoscale vortex in association with a Mesoscale Convective System (MCS) is beyond the scope of the cloud and moisture treatments in the current models.

Based on this framework for understanding the problem, the main physical ideas or concepts in tropical cyclone formation will be summarized. This overview is necessarily selective. Given that a complete theory is not available, the most fundamental processes are not yet known.

3.6.1 Conditional Instability of the Second Kind (CISK)

The basic theoretical framework for many research studies of tropical cyclone formation (e.g., Syono and Yamasaki 1966; Charney 1973a, b; Bates 1973; Koss 1976; Mak 1981; Fraedrich and McBride 1989; Wiin-Nielsen 1993) has been the CISK theory. The basic concept is that the cyclones arise from a hydrodynamic instability produced by gravitational and Coriolis forces that utilizes the latent heat energy released through condensation. Although CISK depends on the release of latent heat in a conditionally unstable atmosphere, it is distinctly different from the ordinary conditional instability that is responsible for the growth of the cumulus clouds. Three basic assumptions are made: (i) the initial perturbation is a synoptic-scale wave with quasi-geostrophic or "balanced" dynamics such that boundary layer convergence occurs in regions of low-level cyclonic vorticity; (ii) latent heat release will occur in the free atmosphere above these regions of frictionally-induced upward motion; and (iii) the magnitude of this heat release is proportional to the Ekman pumping. A feedback loop occurs (Fig. 3.22) in the regions of low-level cyclonic vorticity where upward motion is forced at the top of the boundary layer due to Ekman-induced frictional convergence. The latent heat release that occurs in the free atmosphere aloft induces (or is balanced by) an in-up-out secondary circulation through the processes described by the Eliassen balanced vortex equation (Chapter 2, equation 2.19). The low-level vorticity is then increased by vortex tube stretching due to the inward flow occurring above the boundary layer. Since this increase in low-level vorticity will be accompanied by an increase in Ekman pumping and an increase in latent heat release, a positive feedback loop exists. According to Yamasaki (1988), the key to understanding CISK is the mechanism(s) by which cumulus convection is organized, and convective activity is maintained, for a long period of time. In this context, the basic idea in the CISK theory is that the convection is organized by frictional convergence.

A related instability known as Wave-CISK was developed by Yamasaki (1969), Hayashi (1970), Lindzen (1974), and others. As shown in Fig. 3.23, this mechanism also assumes that the latent heat release in the free atmosphere is governed by convergence at low levels. In this case, the organization of the convergence is governed by the ascending motion incorporated in the dynamics of an equatorial wave mode. Bolton (1980) demonstrated that the instability is mathematically equivalent to large-scale convective overturning (i.e., conditional instability of the first kind). The difference is that the vertical structure of the unstable waves gives a complex (or phase-lagged) form to the heating. Thus, Wave-CISK modes are amplified and also propagated, owing to the phase shift between vertical velocity and heating.

As shown by Hayashi (1970) and Lindzen (1974), this parameterization leads to an unstable (growing) mode for all wave-forms on the dispersion diagram for the equatorial β-plane. Two applications of Wave-CISK are in the study of squall lines or travelling

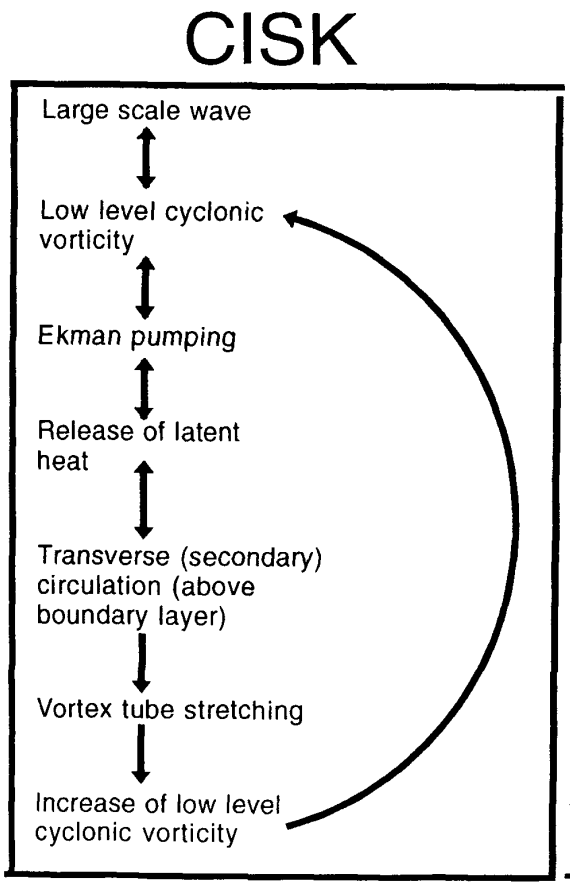

Fig. 3.22 Schematic of the frictional CISK feedback process for a large-scale quasi-geostrophic wave or an initial vortex. In the region of the wave with cyclonic low-level vorticity, Ekman pumping out of the boundary layer is assumed to generate cumulonimbus convection that heats the troposphere. This heating is balanced by a secondary circulation that provides convergence in the lower troposphere, which increases the low-level vorticity through vortex stretching. Because the increased vorticity provides increased Ekman pumping from the boundary layer, a positive feedback loop is established.

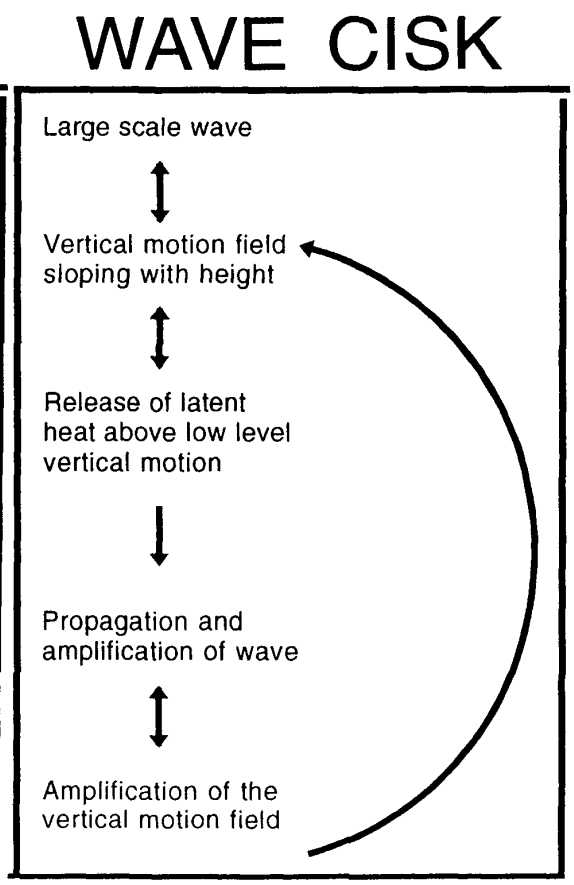

Fig. 3.23 Schematic of Wave-CISK for a wave form with an associated convergence field. In the region of the wave with upward vertical motion at low levels, cumulonimbus convection and latent heat release occurs. Since the wave slopes with height, the maximum heating is out of phase with the maximum vertical motion in the middle troposphere. This configuration causes both propagation and amplification of the wave. The amplification leads to greater vertical motion at low levels, more cumulonimbus heating, etc. to establish a positive feedback loop.

thunderstorm complexes (e.g., Raymond 1984) and studies of the 30-60 day oscillation (e.g., Chang and Lim 1988; Wang and Rui 1990). The major application of Wave-CISK to tropical cyclone formation was by Kurihara and Kawase (1985). Through both linear and nonlinear integrations of a highly simplified numerical model, they demonstrated that the Wave-CISK mechanism can reproduce the transformation of a synoptic wave in the easterlies into a warm-cored closed vortex (Kurihara and Kawase 1985, 1986; McBride and Willoughby 1986).

A third CISK-type instability has been proposed by Fraedrich and McBride (1995). In their mechanism, the heating is parameterized as being proportional to the synoptic-scale vertical motion field with a constant of proportionality equal to the ratio of the cumulonimbus mass flux to the synoptic-scale mass flux. McBride and Fraedrich (1995)

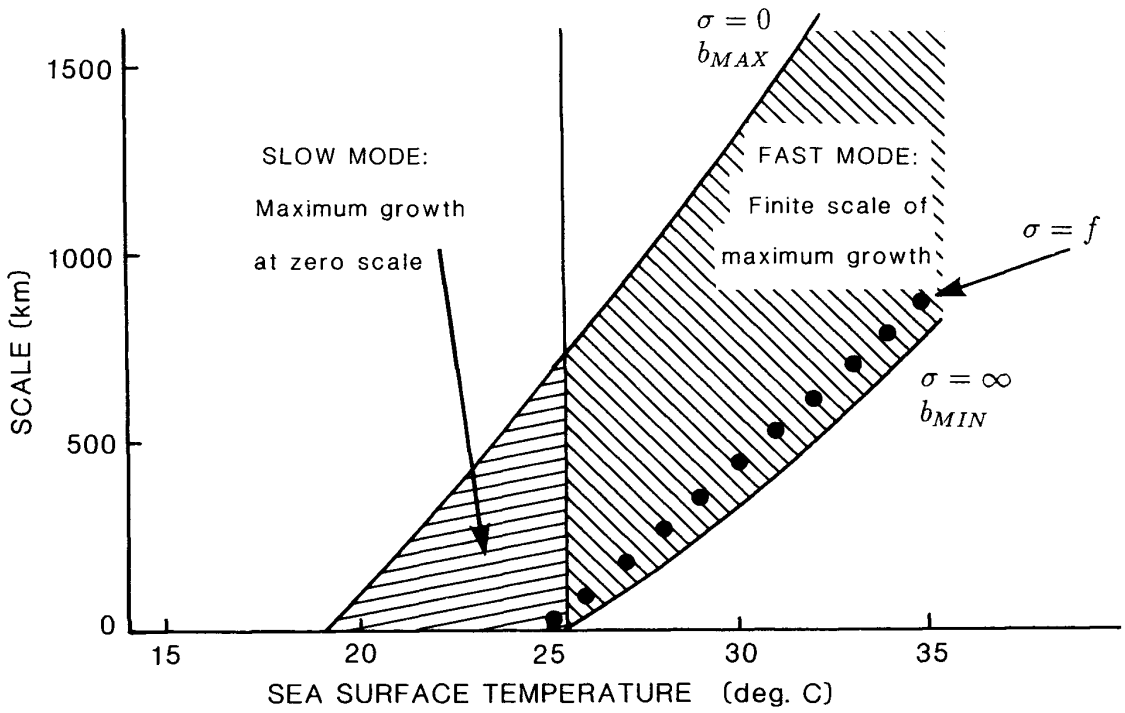

Fig. 3.24 Transition from a slow (CISK) instability to a fast (large-scale overturning) instability at a critical value of sea-surface temperature for the two-layer model of Charney and Eliassen (1964). The shaded region indicates the parameter space with a valid solution (McBride and Fraedrich 1995). At 25.5°C, the fast mode solution sets in with large growth rates at large horizontal scales.

demonstrated this large-scale convective overturning is present in the original two-layer analytical model of Charney and Eliassen (1964). Their model also provides a theory for the rapidly changing response of oceanic tropical convection owing to variations in the sea-surface temperature (Fig. 3.24), which governs the supply of moisture that can be converted into enthalpy through latent heat release. Below a cut-off temperature of 25.5°C, only a slow mode CISK solution is possible. Above this threshold, the fast mode, or large-scale convective overturning, sets in. In this regime, both the growth rate and the horizontal scale of the solution become much larger. Fraedrich and McBride thus propose that this large-scale overturning may be a mechanism for the growth of cloud clusters and pre-cyclone disturbances at sea-surface temperatures exceeding 26°C.

Criticisms of CISK-type instabilities as a mechanism for understanding tropical cyclone formation have been given. Emanuel (1989) states that the CISK models are based on an incorrect assumption that a reservoir of Convective Available Potential Energy (CAPE) exists to drive the large-scale motions. Since CAPE does not appear explicitly in the basic equation set of most CISK models, it is evidently assumed that surface heating and evaporation will maintain the CAPE at the initial value. A weakness of this class of models is that the major component of the physics is in the formulation of the cumulus parameterization, which necessarily contains coefficients dependent on the large-scale moisture field. As shown by Fraedrich and McBride (1995), the solutions vary significantly depending on how the model moisture budget is constructed. Because these theoretical CISK models do not have an explicit (i.e., prognostic) moisture equation, they are incomplete theories.

The original CISK mechanism and the large-scale overturning mechanism are both critically dependent on the Ekman lower boundary condition. Ooyama (1982) and Montgomery and Farrell (1993) noted that the assumed relationship is valid only after an incipient vortex has attained sufficient strength and organization so that the cloud-organizing mesoscale motions are correlated with the larger-scale balanced flow. In the McBride and Fraedrich (1995) model, the scales of preferred growth for the fast mode are

of the order of several hundred kilometers. Thus, a fundamental question is whether tropical motions on that scale may be considered quasi-geostrophic, and particularly whether the Ekman boundary condition is valid on those scales. The validity of CISK-type models depends crucially on this question, which deserves further investigation. In this context, Stout and Young (1983) suggest the low-level flow is quasi-geostrophic beyond about 5 deg. lat. from the equator.

3.6.2 Cyclone development as a response to heating

As discussed in the introduction to this section, when heat is released as rainfall in the tropics there is usually only a very small local response in terms of realized warming or temperature change. The dynamical reason is that the horizontal scale of the heating is small so that gravity wave and other divergent circulations dominate over rotational effects. The relevant horizontal scale is the Rossby deformation radius λ, which (Chapter 2.5.2) is proportional to the ratio of the static stability to the inertial stability, and is a measure of the rotational constraint on the horizontal motion. Schubert *et al.* (1980) studied the geostrophic adjustment to an initial perturbation (analogous to the addition of heat) in an axisymmetric barotropic (i.e., single vertical mode) primitive- equation model. When the heating occurs on a scale much smaller than the deformation radius ($a << 1$), very little of the heat energy remains local to the region of the heating (Fig. 3.25). Conversely, when the heating occurs on horizontal scales such that the rotational constraint is large ($a >> 1$), more of the energy released as heat remains in the form of both kinetic and potential energy in a geostrophically balanced state. According to Schubert and Hack (1982), the normalized scale *a* may be considered as a measure of the *efficiency* of the heating due to cumulonimbus convection.

Related arguments were presented by Ooyama (1982), who noted that when the horizontal scale of the motion is larger than the deformation radius, the flow is essentially horizontal and nearly in geostrophic balance with the pressure field, because of the constraint associated with the background rotation. In the general state of the tropical atmosphere in which disturbances are relatively weak, the rotational constraint arises mainly from the earth's rotation. Thus, the deformation radius λ is effectively equal to *c*,

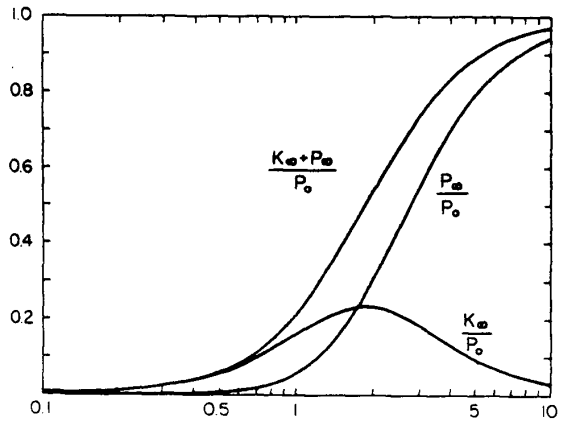

Fig. 3.25 Ratios (ordinate) of the final perturbation kinetic K_{00} and potential P_{00} energies in geostrophic flow to the initial perturbation available potential energy as a function of the horizontal scale normalized by the Rossby deformation radius (abscissa) (Schubert *et al.* 1980).

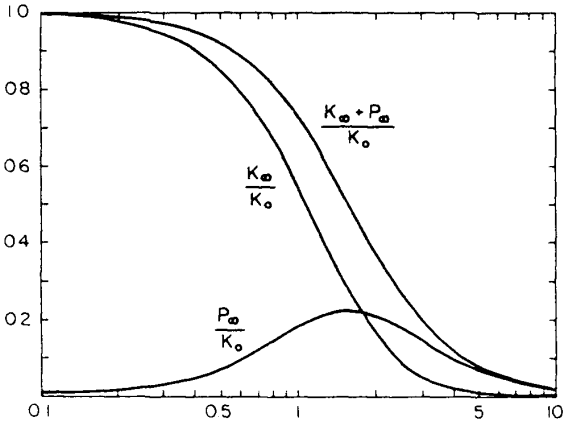

Fig. 3.26 As Fig. 3.25, except that the initial perturbation is in tangential velocity or vorticity.

the phase speed of a pure gravity wave, divided by the Coriolis parameter f. A typical value of λ for the tropics would be 1000 km, which is much larger than the scale of either the individual cumulus elements or of the mesoscale convective elements within the pre-cyclone cloud cluster. Ooyama proposes that since the mesoscale systems occur in the regime $a < 1$, or $l < \lambda$, their evolution is essentially probabilistic, i.e., is not determined by the synoptic-scale, quasi-geostrophic flow. He hypothesizes that the essential question of tropical cyclogenesis is determining the mechanism by which the mesoscale convective systems become under the control of a deterministic environment.

In this context, a number of authors (Ooyama 1982; Schubert and Hack 1982; Shapiro and Willoughby 1982; Hack and Schubert 1986) have proposed that the key to the problem may be that the deformation radius can be modified due to the presence of local regions of cyclonic vorticity ξ. That is, a rotational constraint is provided by the combination of earth plus relative vorticity, so that $\lambda \quad c/(f + \xi)$. Thus, the deformation radius becomes smaller so that the ratio a of the scale of the mesoscale convective systems to the deformation radius approaches one, and the *efficiency* of heating is mainly governed by the distribution of convection relative to variations in inertial stability (Schubert and Hack 1982).

Tropical cyclone formation may be considered as a nonlinear process whereby local warming by cumulus convection and mesoscale elements is enhanced if the convection is confined to regions of relatively high inertial stability. Under these circumstances, the energy released as latent heat can bring about a localized increase in kinetic energy and vorticity, which further increases the local inertial stability, and therefore the "efficiency" of the heating. This process is fundamentally nonlinear in character, which distinguishes it from the CISK models that depend on an instability that is present in the linearized equations.

An alternate method to bring about a localized warming of the tropical atmosphere may be through localized sources of momentum rather than of heat. The redistribution of mass by the secondary circulation exports energy away from the region of heating. Referring to the Eliassen balanced vortex equation (2.19), the secondary circulation is forced by the horizontal gradients in heat sources and by vertical gradients of momentum sources. As shown in Fig. 3.26, the response of the tropical atmosphere to momentum sources has the opposite character to that of heat sources (Fig. 3.25), in that the efficiency of momentum sources in increasing the potential and kinetic energy of the localized flow is very high at scales such that the rotational constraint is weak ($a << l$). Thus, McBride (1981b) and Davidson (1995) have proposed that the initial warming of the atmosphere in cyclone formation may occur in response to the direct modification of the vorticity fields by the cumulonimbus elements.

Another form of direct modification of the momentum fields is through the eddy import of angular momentum through interaction with surrounding upper-level weather systems. This mechanism has been described observationally in Chapter 3.5.7 and theoretically in Chapter 2.4.1.

3.6.3 Recent theories

In a series of papers, Emanuel and co-authors (Emanuel 1989, 1993; Yano and Emanuel 1991; Emanuel *et al.* 1994) proposed that tropical cyclones are formed by a mechanism known as WISHE (wind-induced surface heat exchange). The basic idea is that the latent heat release in the free troposphere is governed by the evaporation of moisture (and therefore moist static energy or θ_E) from the sea, which is primarily determined by the magnitude of the surface winds. Whereas the cumulus parameterization in a simplified WISHE model has heat release proportional to the low- level wind speed, in the CISK models it is proportional to the vorticity, which is effectively the gradient of the low-level wind speed. The WISHE mechanism alone will not bring about amplification of a large-scale, warm-cored vortex, because deep convection initiated through Ekman pumping will typically be accompanied by convective-scale downdrafts that will lower the

moist static energy of the subcloud layer air. This cooling and drying will negate any increase in moist static energy due to the increased surface winds, and the vortex will decay. Based on the observations in the TEXMEX experiment, the additional condition for amplification of an initial vortex is that the troposphere becomes nearly saturated on the mesoscale in the vortex core (Emanuel 1989). That is, the mid-tropospheric minimum in moist static energy must be reduced so that evaporation of rain does not generate downdrafts that import cool, dry air to the subcloud layer. Thus, the enhanced surface fluxes associated with the strong surface winds near the core can increase the subcloud moist static energy and through convection can increase the temperature of the vortex core. In a moist tropical atmosphere, the WISHE process can thus act as a positive feedback to the warm-core cyclone (Emanuel *et al.* 1994).

Recall the formation of the initial disturbance is accompanied by a large-scale spin-up, which may be governed by large-scale barotropic dynamics. Guinn and Schubert (1993) proposed that a zonally elongated monsoon trough with low-level easterlies on the poleward side and low-level westerlies on the equatorward side may be considered as a zonal strip of high potential vorticity PV. The associated meridional gradients of PV can support a PV wave on the equatorward edge of the strip that will propagate westward relative to the westerly flow and a PV wave on the poleward edge that will propagate eastward relative to the easterly flow. Guinn and Schubert propose these two counter-

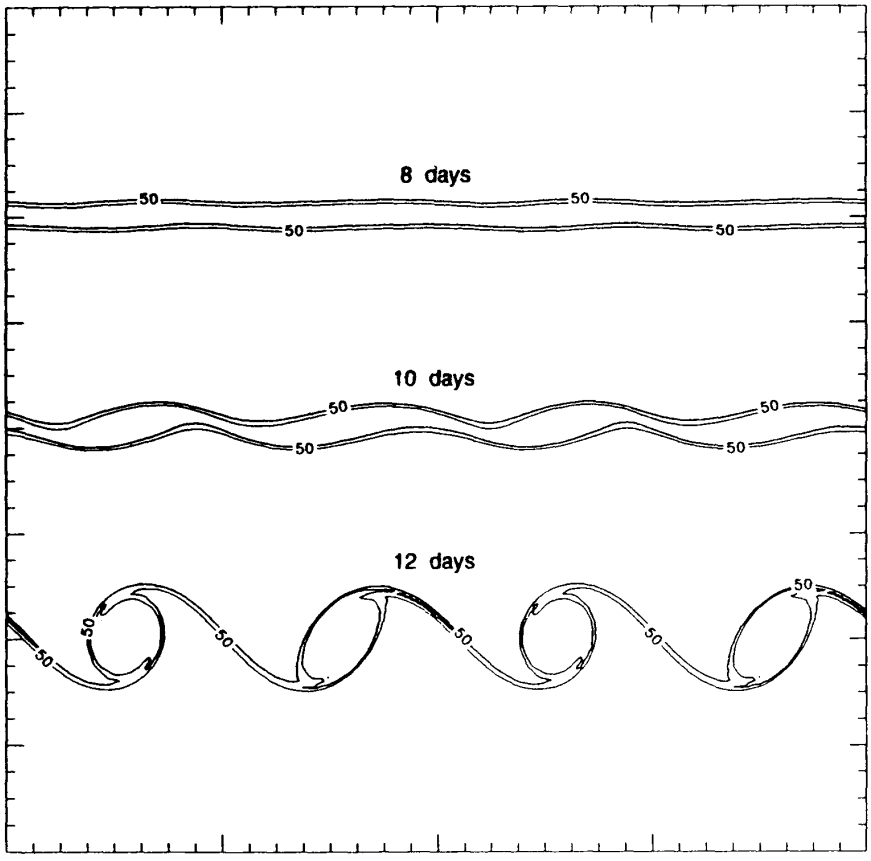

Fig. 3.27 Schematic of breakdown of the ITCZ into discrete vortices as simulated by Guinn and Schubert (1993) model. Contours are of vorticity at 8, 10, and 12 days into the simulation. Tick marks along the boundaries are at 400 km.

propagating PV waves may have the same phase speed relative to the earth such a phase-locking will be favorable for mutual growth of the waves, and barotropic instability may result (Hoskins *et al.* 1985). The subsequent "ITCZ breakdown" leads to a pooling of PV into regions connected by filaments (Fig. 3.27). These pools become more axisymmetric and the filaments become elongated and start to wrap around the PV centers. Some observations similar to this breakdown of the ITCZ into discrete vortices are discussed by Guinn and Schubert. McBride (1986) had earlier proposed that two distinct modes of monsoon trough convective organization exist (Fig. 3.28). Active type 1 has the convection organized on the 30 deg. long. super-cluster scale (e.g., McBride 1983; Keenan and Brody 1988). In Active type 2, the monsoon trough is broken into a number of discrete convective systems that may be associated with either a tropical cyclone or a monsoon depression.

Another explanation for alternating convection and relatively cloud-free areas within the monsoon trough is the eastward energy dispersion mechanism of Davidson and Hendon, discussed observationally in Chapter 3.5.3. Chang *et al.* (1995) investigated this mechanism using a barotropic vorticity model to simulate the propagation of a large- scale vortex in a monsoon shear. The vortex develops a westward and poleward propagation and an energy dispersion due to a nonlinear Rossby (advection plus beta) effect. Since the energy dispersion is equatorward and eastward, a trailing wake of anticyclones and cyclones is established, which could lead to suppressed and enhanced convective areas as observed by Davidson and Hendon (1989), Davidson *et al.* (1990), and McBride *et al.* (1995).

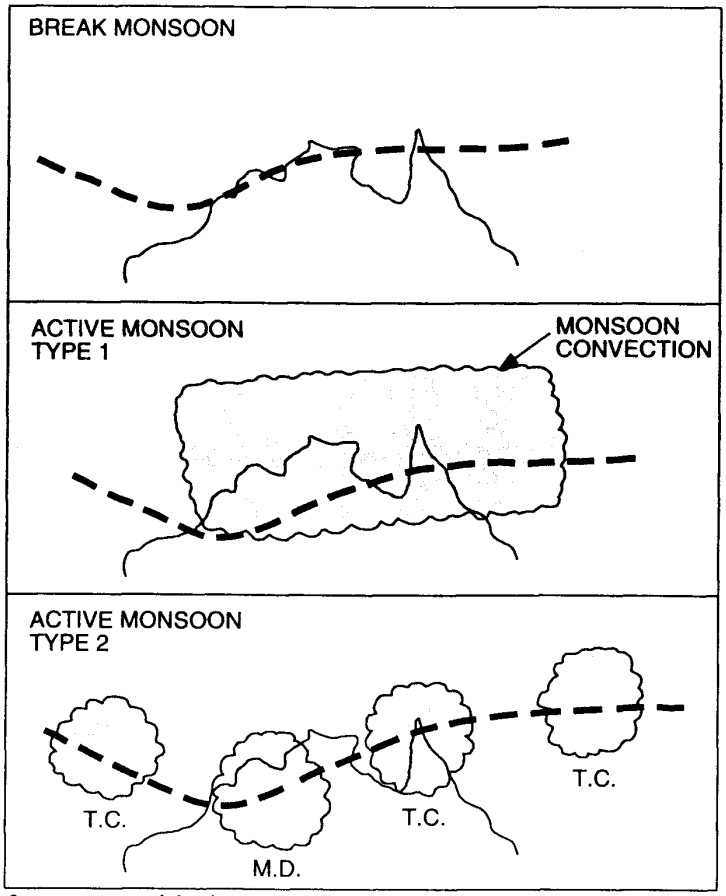

Fig. 3.28 Separation of monsoon activity into a break phase and two active phases as proposed by McBride (1986). The dashed line is the location of the monsoon trough. The shaded area depicts the cumulonimbus activity, and T.C. and M.D. are tropical cyclones and monsoon depressions.

As a final comment, tropical cyclone formation is currently a rich area for observational, theoretical, and numerical research. As discussed by Ooyama (1982) and Emanuel *et al.* (1994), the CISK theory of the 1960's dominated thinking on the problem to such an extent that it possibly impeded progress. Although alternate frameworks for understanding the problem have emerged, the new theories also have not easily explained either the relative rareness of tropical cyclone formation or its strong control by the large-scale influences discussed in Chapter 3.4.

REFERENCES

Allard, R. A., 1984: A climatology of the characteristics of tropical cyclones in the Northeast Pacific during the period of 1966-1980. Master of Science Thesis, Texas Tech. Univ., Lubbock, TX, 106 pp.

Anthes, R. A., 1982: Tropical cyclones: Their evolution, structure and effects. *Meteor. Monogr.*, **41**, Amer. Meteor. Soc., Boston, MA 02108, 208 pp.

Atkinson, G. D., 1971: Forecaster's guide to tropical meteorology. Technical Report 240. United States Air Force, Air Weather Service, 350 pp.

Avila, L. A., 1991: Eastern North Pacific hurricane season of 1990. *Mon. Wea. Rev.*, **119**, 2034-2051.

Ballenzweig, E., 1959: Relation of long-period circulation anomalies to tropical cyclone formation and motion. *J. Meteor.*, **16**, 121-188.

Bates, J. R., 1973: A generalization of the CISK theory. *J. Atmos. Sci.*, **30**, 1509-1519.

Bath, A. T., S. H. Lloyd, and P. Ryan, 1956: Practical techniques used in the Australian region for tropical cyclone forecasting. *Proc. Trop. Cycl.. Symp., Brisbane*, Australian Bureau of Meteorology, 121-133.

Bolton, D., 1980: Application of the Miles theorem to forced linear perturbations. *J. Atmos. Sci.*, **37**, 1639-1642.

Bosart, L. R., and F. Sanders, 1981: The Johnstown flood of July 1987: A long-lived convective storm. *J. Atmos. Sci.*, **38**, 1616-1642.

Brandes, E. A., 1990: Evolution and structure of the 6-7 May 1985 mesoscale convective system and associated vortex. *Mon. Wea. Rev.*, **118**, 109-127.

Bureau of Meteorology, 1978: *The Australian Tropical Cyclone Forecasting Manual.* Bureau of Meteorology, P. O. Box 1289K, Melbourne, Victoria 3001, Australia, 274 pp.

Chan, J. C.-L., 1985: Tropical cyclone activity in the northwest Pacific in relation to the El Nino/Southern Oscillation phenomenon. *Mon. Wea. Rev.*, **113**, 599-606.

Chang, C.-P., and H. Lim, 1988: Kelvin wave-CISK: A possible mechanism for the 30 - 50 day oscillation. *J. Atmos. Sci.*, **45**, 1709-1720.

Chang, C.-P., J.-M. Chen, P. A. Harr, and L. E. Carr, 1995: Northwestward propagating synoptic wave patterns over the tropical western Pacific and the periodicity of tropical cyclone activity. Submitted to *Mon. Wea. Rev.*

Charney, J. G., 1963: A note on the large-scale motions in the tropics. *J. Atmos. Sci.*, **20**, 607-609.

Charney, J. G., 1973a: Moveable CISK. *J. Atmos. Sci.*, **30**, 50-52.

Charney, J. G., 1973b: Planetary fluid dynamics. *Dynamical Meteorology*, P. Morel, (Ed.) Reidel Publ., 331-344.

Charney, J. G., and A. Eliasen, 1964: On the growth of the hurricane depression. *J. Atmos. Sci.*, **41**, 901-924.

Chen, L. S., and Y. W. Ding, 1979: *A General Introduction to Tropical Cyclones in the Western Pacific.* Academy Press, Beijing, 491 pp.

Chen, S. A., and W. M. Frank, 1993: A numerical study of the genesis of extratropical convective mesovortices. Part I. Evolution and dynamics. *J. Atmos. Sci.*, **50**, 2401-2426.

Davidson, N. E., 1995: Vorticity budget for AMEX. Part I. Diagnostics. *Mon. Wea. Rev.*, **123**, 1620-1635.

Davidson, N. E., and G. J. Holland, 1987: A diagnostic analysis of two intense monsoon depressions over Australia. *Mon. Wea. Rev.*, **115**, 380-392.

Davidson, N. E., and H. H. Hendon, 1989: Downstream development in the Southern Hemisphere monsoon during FGGE/WMONEX. *Mon. Wea. Rev.*, **117**, 1458-1470.

Davidson, N. E., and A. Kumar, 1990: Numerical simulation of the development of AMEX tropical cyclone Irma. *Mon. Wea. Rev.*, **118**, 2001-2019.

Davidson, N. E., G. J. Holland, J. L. McBride, and T. D. Keenan, 1990: On the formation of AMEX tropical cyclones Irma and Jason. *Mon. Wea. Rev.*, **118**, 1981-2000.

Dong, K.-Q., 1988: El Nino and tropical cyclone frequency in the Australian region and the Northwest Pacific. *Aust. Meteor. Mag.*, **36**, 219-225.

Dunnavan, G. M., R. L. Elsberry, P. A. Harr, E. J. McKinley, and M. A. Boothe, 1993: Overview of the tropical cyclone motion - 92 (TCM-92) mini-field experiment. *Preprints, 20th Conf. Hurr. Trop. Meteor.*, San Antonio, TX, Amer. Meteor. Soc., Boston, MA 02108, 477-480.

Dvorak, V. F., 1975: Tropical cyclone intensity analysis and forecasting from satellite imagery. *Mon. Wea. Rev.*, **103**, 420-430.

Dvorak, V. F., 1984: Tropical cyclone intensity analysis using satellite data. NOAA Technical Report NESDIS 11, U. S. Dept. of Commerce, Washington, DC, 47 pp.

Emanuel, K. A., 1989: The finite-amplitude nature of tropical cyclogenesis. *J. Atmos. Sci.*, **46**, 3431-3456.

Emanuel, K. A., 1993: The physics of tropical cyclogenesis over the Eastern Pacific. *Tropical Cyclone Disasters.* J. Lighthill, Z. Zhemin, G. J. Holland, K. Emanuel (Eds.), Peking University Press, Beijing, 136-142.

Emanuel, K. A., N. Renno, L. R. Schade, M. Bister, M. Morgan, D. J. Raymond, and R. Rotunno, 1993: Tropical cyclogenesis over the eastern North Pacific: Some results from TEXMEX. *Preprints, 20th Conf. Hurr. Trop. Meteor.*, San Antonio, TX, Amer. Meteor. Soc., Boston, MA 02108, 110-113.

Emanuel, K. A., J. D. Neelin, and C. S. Bretherton, 1994: On large-scale circulations in convecting atmospheres. *Quart. J. Roy. Meteor. Soc.*, **120**, 1111-1143.
Evans, J. L., and R. J. Allen, 1992: El Nino/Southern Oscillation modification to the structure of the monsoon and tropical activity in the Australian region. *Intl. J. Climatology*, **12**, 611-623.
Fett, R. W., 1966: Upper level structure of the formative tropical cyclone. *Mon. Wea. Rev.*, **94**, 9-15.
Fett, R. W., 1968: Typhoon formation within the zone of the intertropical convergence. Mon. Wea. Rev., **96**, 106-117.
Fiorino, M. J., S. Goerss, J. J. Jensen, and E. J. Harrison, Jr., 1993: An evaluation of the real-time tropical cyclone forecast skill of the Navy operational global atmospheric prediction system in the western North Pacific. *Wea. and Forecasting*, **8**, 3-24.
Fraedrich, K., and J. L. McBride, 1989: The physical mechanism of CISK and the free-ride balance. *J. Atmos. Sci.*, **46**, 2642-2648.
Fraedrich, K., and J. L. McBride, 1995: Large scale convective instability revisited. *J. Atmos. Sci.*, **52**, 1914-1923.
Frank, W. M., 1982: Large-scale characteristics of tropical cyclones. *Mon. Wea. Rev.*, **110**, 572-586.
Frank, W. M., 1987: Tropical cyclone formation. Chap. 3, *A Global View of Tropical Cyclones*. Office of Naval Research, Arlington, VA 22217, 53-90.
Frank, W. M., and S. Chen, 1991: Simulations of vortex formation in convective weather systems. *Preprints, 19th Conf. Hurr. Trop. Meteor.*, Miami, FL, Amer. Meteor. Soc., Boston, MA 02108, 241-244.
Fritsch, J. M., and R. A. Maddox, 1981: Convectively driven mesoscale weather systems aloft. *J. Appl. Meteor.*, **20**, 9-19.
Gray, W. M., 1968: Global view of the origin of tropical disturbances and storms. *Mon. Wea. Rev.*, **96**, 669-700.
Gray, W. M., 1975: Tropical cyclone genesis. Dept. of Atmos. Sci. Paper No. 323, Colorado State University, Ft. Collins, CO 80523, 121 pp.
Gray, W. M., 1979: Hurricanes: Their formation, structure and likely role in the tropical circulation. *Meteorology Over the Tropical Oceans*. D. B. Shaw (Ed.), Roy. Meteor. Soc., James Glaisher House, Grenville Place, Bracknell, Berkshire, RG12 1BX, 155-218.
Gray, W. M., 1984a: Atlantic seasonal hurricane frequency. Part I: El Nino and 30 mb QBO influences. *Mon. Wea. Rev.*, **112**, 1649-1668.
Gray, W. M., 1984b: Atlantic seasonal hurricane frequency. Part II. Forecasting its variability. *Mon. Wea. Rev.*, **112**, 1669-1683.
Gray, W. M., 1985: Tropical cyclone global climatology. Technical Document WMO/TD-No. 72, Vol. 1, World Meteorological Organization, Geneva, Switzerland, 3-19.
Gray, W. M., 1990: Strong association between West African rainfall and U. S. landfall of intense hurricanes. *Science*, **279**, 1251- 1256.
Gray, W. M., C. W. Landsea, P. Mielke, and K. Berry, 1992: Predicting Atlantic seasonal hurricane activity 6-11 months in advance. *Wea. and Forecasting*, **7**, 440-455.
Gray, W. M., C. W. Landsea, P. W. Mielke, and K. J. Berry, 1993: Predicting Atlantic basin seasonal tropical cyclone activity by 1 August. *Wea. Forecasting*, **8**, 73-86.
Guinn, T. A., and W. H. Schubert, 1993: Hurricane spiral bands. *J. Atmos. Sci.*, **50**, 3380-3408.
Hack, J. J., and W. H. Schubert, 1986: Nonlinear response of atmospheric vortices to heating by organized cumulus convection. *J. Atmos. Sci.*, **43**, 1559-1573.
Hastings, P. A., 1990: Southern Oscillation influences on tropical cyclone activity in the Australian/Southwest Pacific region. *Intl. J. Climatology*, **10**, 291-298.
Hayashi, Y., 1970: A theory of large-scale equatorial waves generated by condensation heat and accelerating the zonal wind. *J. Meteor. Soc. Japan*, **48**, 140-160.
He, S. W., and Z. F. Yang, 1981: The relationship between the intensity of summer southwest monsoon over the northwest Pacific and the circulation patterns of the Southern Hemisphere. *Scientia Atmospheric Sinica*, **5**, 50-59.
Hebert, P. J., and G. Taylor, 1983: The deadliest, costliest, and most intense United States hurricanes of this century (and other frequently requested hurricane facts). NOAA Tech Memo. NWD NHC 18, National Hurricane Center, Coral Gables, FL 33146, 25 pp.
Holland, G. J., 1983: Angular momentum transports in tropical cyclones. *Quart. J. Roy. Meteor. Soc.*, **109**, 187-209.
Holland, G. J., 1984a: On the climatology and structure of tropical cyclones in the Australian/Southwest Pacific region. I. Data and tropical storms. *Aust. Meteor. Mag.*, **32**, 1-16.
Holland, G. J., 1984b: On the climatology and structure of tropical cyclones in the Australian/Southwest Pacific region. II. Hurricanes. *Aust. Meteor. Mag.*, **32**, 17-32.
Holland, G. J., 1984c: On the climatology and structure of tropical cyclones in the Australian/Southwest Pacific region. III. Major hurricanes. *Aust. Meteor. Mag.*, **32**, 33-46.
Hoskins, B. J., M. E. McIntyre, and A. W. Robertson, 1985: On the use and significance of isentropic potential vorticity maps. *Quart. J. Roy. Meteor. Soc.*, **111**, 877-946.
Houze, R. A., Jr., S. G. Geotis, F. D. Marks, and A. K. West, 1981: Winter monsoon convection in the vicinity of north Borneo. Part I: Structure and time variation of the clouds and precipitation. *Mon. Wea. Rev.*, **108**, 1595-1614.
Hubert, L. F., 1955: A case study of hurricane formation. *J. Meteor.*, **12**, 486-492.
Johnson, R. H., and R. A. Houze, 1987: Precipitation cloud systems of the Asian monsoon. In *Monsoon Meteorology*, C.-P. Chang and T. N. Krishnamurti (Eds.), Oxford University Press, 298-353.
Keen, R. A., 1982: The role of cross-equatorial tropical cyclone pairs in the Southern Oscillation. *Mon. Wea. Rev.*, **110**, 1405-1416.
Keenan, T. D., and L. R. Brody, 1988: Synoptic-scale modulation of convection during the Australian summer monsoon. *Mon. Wea. Rev.*, **116**, 71-85.

Coss, W. J., 1976: Linear stability analysis of CISK-induced disturbances: Fourier component eigenvalue analysis. *J. Atmos. Sci.*, **33**, 1195-1222.
Crishnamurti, T. N., H. S. Bedi, D. Oosterhof, and V. Hardiker, 1994: The formation of hurricane Fredric of 1979. *Mon. Wea. Rev.*, **122**, 1050-1074.
Curihara, Y., and M. Kawase, 1985: On the transformation of a tropical easterly wave into a tropical depression: A simple numerical study. *J. Atmos. Sci.*, **42**, 68-77.
Curihara, Y., and M. Kwase, 1986: Reply. *J. Atmos. Sci.*, **43**, 3284-3286.
Kuo, H. L., 1965: On formation and intensification of tropical cyclones through latent heat release by cumulus convection. *J. Atmos. Sci.*, **22**, 40-63.
Kuo, Y. H., L. S. Cheng, and R. A. Anthes, 1985: Mesoscale analysis of Sichuan flood catastrophe, 11-15 July 1981. *Mon. Wea. Rev.*, **114**, 1503-1527.
Lander M. A., 1990: Evolution of the cloud pattern during the formation of tropical cyclone twins symmetrical with respect to the equator. *Mon. Wea. Rev.*, **118**, 1194-1202.
Lander, M. A., 1994: An exploratory analysis of the relationship between tropical storm formation in the Western North Pacific and ENSO. *Mon. Wea. Rev.*, **122**, 636-651.
Landsea, C. W., and W. M. Gray, 1992: The strong association between western Sahelian monsoon rainfall and intense Atlantic hurricanes. *J. Climate*, **5**, 435-453.
Lau, K. M., T. Nakazawa, and C. H. Sui, 1991: Observations of cloud cluster hierarchies over the tropical western Pacific. *J. Geophys. Res.*, **96**, 3197-3208.
Leary, C. A., and E. N. Rappaport, 1987: The life cycle and internal structure of a mesoscale convective complex. *Mon. Wea. Rev.*, **115**, 1503-1527.
Lee, C.-S., 1989: Observational analysis of tropical cyclogenesis in the western North Pacific. Part I. Structural evolution of cloud clusters. *J. Atmos. Sci.*, **46**, 2580-2598.
Liebmann, B., H. H. Hendon, and J. D. Glick, 1994: The relationship between tropical cyclones of the western Pacific and Indian Oceans and the Madden-Julian oscillation. *J. Meteor. Soc. Japan*, **72**, 401-412.
Lindzen, R. S., 1974: Wave-CISK in the tropics. *J. Atmos. Sci.*, **31**, 156-179.
Lopez, L., D. Raymond, and K. Emanuel, 1993: Preliminary results from TEXMEX: The development of tropical storm Guillermo. *Preprints, 20th Conf. Hurr. Trop. Meteor.*, San Antonio, TX, Amer. Meteor. Soc., Boston, MA 02108, 114-117.
Love, G., 1985a: The role of the general circulation in western Pacific tropical cyclone genesis. Atmos. Sci. Paper No. 340, Colorado State University, Ft. Collins, CO 80523, 215 pp.
Love, G., 1985b: Cross-equatorial influence of winter hemisphere subtropical cold surges. *Mon. Wea. Rev.*, **113**, 1487-1498.
Maddox, R. A., 1980: Mesoscale convective complexes. *Bull. Amer. Meteor. Soc.*, **61**, 1374-1387.
Mak, M.-K., 1981: An inquiry on the nature of CISK, Part I. *Tellus*, **33**, 531-537.
Mandal, G. S., and C. J. Neumann, 1976: Climatology of North Indian Ocean tropical cyclones by 2 1/2 degree latitude-longitude squares. Fellowship report of senior author, submitted to *India Meteorological Dept.*
Manton, M. J., and J. L. McBride, 1992: Recent research on the Australian Monsoon. *J. Meteor. Soc. Japan*, **70**, 275-285.
Mayfield, M., and M. B. Lawrence, 1991: Atlantic hurricane season of 1990. *Mon. Wea. Rev.*, **119**, 2014-2026.
McBride, J. L., 1981a: Observational analysis of tropical cyclone formation. Part I. Basic definition of data sets. *J. Atmos. Sci.*, **38**, 1117-1131.
McBride, J. L., 1981b: Observational analysis of tropical cyclone formation. Part III. Budget analysis. *J. Atmos. Sci.*, **38**, 1152-1156.
McBride, J. L., 1983: Satellite observations of the Southern Hemisphere monsoon during winter MONEX. *Tellus*, **35A**, 189-197.
McBride, J. L., 1986: Tropical cyclones in the Southern Hemisphere summer monsoon. *Second Intl. Conf. Southern Hemisphere Meteor.*, Amer. Meteor. Soc., Boston, MA 02108, 358-364.
McBride, J. L., and W. M. Gray, 1980: Mass divergence in tropical weather systems. Part I: Diurnal variation. *Quart. J. Roy. Meteor. Soc.*, **106**, 501-516.
McBride, J. L., and R. Zehr, 1981: Observational analysis of tropical cyclone formation. Part II: Comparison of non-developing versus developing systems. *J. Atmos. Sci.*, **38**, 1132-1151.
McBride, J. L., and T. D. Keenan, 1982: Climatology of tropical cyclone genesis in the Australian region. *J. Climat.*, **2**, 13-33.
McBride, J. L., and H. E. Willoughby, 1986: Comment-An interpretation of Kurihara and Kawase's two-dimensional tropical cyclone development model. *J. Atmos. Sci.*, **43**, 3279-3283.
McBride, J. L., and G. J. Holland, 1989: The Australian monsoon experiment (AMEX): Early results. *Aust. Meteor. Mag.*, **37**, 23-35.
McBride, J. L., N. E. Davidson, and K. Puri, 1993: An evaluation of the skill of a real-time large-scale NWP model at predicting tropical cyclone development. Presented at *20th Conf. Hurr. and Trop Meteor.*, San Antonio, TX, Amer. Meteor. Soc., Boston, MA 02108.
McBride, J. L., and K. Fraedrich, 1995: CISK: A theory for the response of tropical convective complexes to variations in sea surface temperature. *Quart. J. Roy. Meteor. Soc.*, **121**, (in press).
McBride, J. L., N. E. Davidson, K. Puri, and G. C. Tyrell, 1995: The flow during TOGA-COARE as diagnosed by the BMRC tropical analysis and prognosis scheme. *Mon. Wea. Rev.*, **123**, (in press).
McKinley, E. J., and R. L. Elsberry, 1993: Observations during TCM-92 of the role of tropical mesoscale convective systems in tropical cyclogenesis. *Preprints, 20th Conf. Hurr. Trop. Meteor.*, San Antonio, TX, Amer. Meteor. Soc., Boston, MA 02108, 401-404.
McRae, J. N., 1956: The formation and development of tropical cyclones during the 1955-1956 summer in Australia. *Proc. Trop. Cyc. Symp.*, Brisbane, Bureau of Meteorology, P. O. Box 1289K, Melbourne, Victoria 3001, Australia, 233-262.

Menard, R. D., and J. M. Fritsch, 1989: A mesoscale convective complex-generated inertially stable warm core vortex. *Mon. Wea. Rev.*, **117**, 1237-1261.
Miller, D., and J. M. Fritsch, 1991: Mesoscale convective complexes in the western Pacific region. *Mon. Wea. Rev.*, **119**, 2978-2991.
Montgomery, M. T., and B. F. Farrell, 1993: Tropical cyclone formation. *J. Atmos. Sci.*, **50**, 285-310.
Namias, J., 1955: Secular fluctuations in vulnerability of tropical cyclones in and off New England. *Mon. Wea. Rev.*, **83**, 155-162.
Neumann, C. J., 1993: Global overview. Chap. 1, *Global Guide to Tropical Cyclone Forecasting.* World Meteor. Organization, Geneva, Switzerland, 1.1-1.56.
Neumann, C. J., B. R. Jarvinen, C. J. McAdie, and J. D. Elms, 1993: Tropical cyclones of the North Atlantic Ocean, 1871-1992. *Historical Climatology Series* 6-2, NOAA, Asheville, NC, 193 pp.
Nicholls, N., 1979: A possible method for predicting seasonal tropical cyclone activity in the Australian region. *Mon. Wea. Rev.*, **107**, 1221-1224.
Nicholls, N., 1984: The Southern Oscillation, sea-surface temperature, and interannual fluctuations in Australian tropical cyclone activity. *J. Climatol.*, **4**, 661-670.
Nicholls, N., 1985: Predictability of interannual variations of Australian seasonal tropical cyclone activity. *Mon. Wea. Rev.*, **113**, 1144-1149.
Nicholls, N., 1992: Recent performance of a method for forecasting Australian seasonal tropical cyclone activity. *Aust. Meteor. Mag.*, **21**, 105-110.
Ogura, Y., 1964: Frictionally controlled, thermally driven circulations in a circular vortex with application to tropical cyclones. J. Atmos. Sci., 21, 610-621.
Ooyama, K. V., 1964: A dynamical model for the study of tropical cyclone development. *Geofis. Int.*, **4**, 187-198.
Ooyama, K. V., 1982: Conceptual evolution of the theory and modeling of the tropical cyclone. *J. Meteor. Soc. Japan*, **60**, 369-380.
Palmen, E., 1956: A review of knowledge on the formation and development of tropical cyclones. *Proc. Trop. Cyc. Symp.*, Brisbane, Australian Bureau of Meteorology, P. O. Box 1289K, Melbourne, Victoria 3001, Australia, 213-232.
Pasch, R. J., and L. A. Avila, 1992: Atlantic hurricane season of 1992. *Mon. Wea. Rev.*, **120**, 2671-2687.
Puri, K., and M. J. Miller, 1990: Sensitivity of ECMWF analyses-forecasts of tropical cyclones to cumulus parameterization. *Mon. Wea. Rev.*, **118**, 1709-1741.
Ramage, C. S., 1974: The typhoons of October 1970 in the South China Sea: Intensification, decay and ocean interaction. *J. Appl. Meteor.*, **13**, 739-751.
Ramage, C. S., 1986: El Nino. *Sci. Amer.*, **254**, 76-83.
Raper, S., 1992: Observational data on the relationships between climatic change and the frequency and magnitude of severe tropical storms. In *Climate and sea level change: Observations, projections and implications*, R. A. Warrick, E. M. Barrow, and T. M. L. Wigley (Eds.) Cambridge University Press, 192-212.
Raymond, D. J., 1984: A wave-CISK model of squall lines. *J. Atmos. Sci.*, **41**, 1946-1958.
Revell, C. G., and S. W. Goulter, 1986a: South Pacific tropical cyclones and the Southern Oscillation. *Mon. Wea. Rev.*, **114**, 1138-1145.
Revell, C. G., and S. W. Goulter, 1986b: Lagged relations between the Southern Oscillation and numbers of tropical cyclones in the South Pacific region. *Mon. Wea. Rev.*, **114**, 2669-2670.
Riehl, H., 1948: On the formation of typhoons. *J. Meteor.*, **5**, 247-264.
Riehl, H., 1954: *Tropical Meteorology.* McGraw-Hill, New York, 392 pp.
Riehl, H., 1979: *Climate and Weather in the Tropics.* Academic Press, 611 pp.
Ritchie, E. A., 1993: Contributions by mesoscale convective systems to the formation of tropical cyclones. *Preprints, 20th Conf. Hurr. Trop. Meteor.*, San Antonio, TX, Amer. Meteor. Soc., Boston, MA 02108, 409-412.
Ritchie, E. A., G. J. Holland, and M. Lander, 1993: Contributions by mesoscale convective systems to movement and formation of tropical cyclones. *Tropical Cyclone Disasters*, J. Lighthill, Z. Zhemin, G. J. Holland, and K. Emanuel (Eds.), Peking University Press, Beijing, 286-289.
Ruprecht, E., and W. M. Gray, 1976a: Analysis of satellite-observed cloud clusters. Part I. Wind and dynamic fields. *Tellus*, **28**, 391-413.
Ruprecht, E., and W. M. Gray, 1976b: Analysis of satellite-observed cloud clusters. Part II: Thermal, moisture and precipitation. *Tellus*, **28**, 414-426.
Sadler, J. C., 1976: A role of the tropical upper tropospheric trough in early season typhoon development. *Mon. Wea. Rev.*, **104**, 1266-1278.
Sadler, J. C., 1978: Mid-season typhoon development and intensity changes and the tropical upper tropospheric trough. *Mon. Wea. Rev.*, **106**, 1137-1152.
Schubert, W. H., J. J. Hack, P. L. Silva Dias, and S. R. Fulton, 1980: Geostrophic adjustment in an axisymmetric vortex. *J. Atmos. Sci.*, **37**, 1464-1484.
Schubert, W. H., and J. J. Hack, 1982: Inertial stability and tropical cyclone development. *J. Atmos. Sci.*, **39**, 1688-1697.
Scrinivasan, V., and K. Ramanamurty, 1973: Forecasting Manual, III-4. *India Meteorological Department*, New Delhi, India.
Shapiro, L. J., 1982a: Hurricane climatic fluctuations: Part I: Patterns and cycles. *Mon. Wea. Rev.*, **110**, 1007-1013.
Shapiro, L. J., 1982b: Hurricane climatic fluctuations. Part II: Relation to the large-scale circulation. *Mon. Wea. Rev.*, **110**, 1014-1040.
Shapiro, L. J., 1987: Month-to-month variability of the Atlantic tropical circulation and its relationship to tropical cyclone formation. *Mon. Wea. Rev.*, **115**, 2598-2614.

Shapiro, L. J., 1989: The relationship of the Quasi-Biennial Oscillation to Atlantic tropical storm activity. *Mon. Wea. Rev.*, **117**, 1545-1552.
Shapiro, L. J., and H. E. Willoughby, 1982: The response of balanced hurricanes to local sources of heat and momentum., *J. Atmos. Sci.*, **39**, 378-394.
Simpson, R. H., N. Frank, D. Shideler, and H. M. Johnson, 1969: Atlantic tropical disturbances of 1968. *Mon. Wea. Rev.*, **97**, 240-255.
Steranka, J., E. B. Rodgers, and R. C. Gentry, 1986: The relationship between satellite measured convective bursts and tropical cyclone intensification. *Mon. Wea. Rev.*, **114**, 1539-1546.
Stout, J. E., and J. A. Young, 1983: Low-level monsoon dynamics derived from satellite winds. *Mon. Wea. Rev.*, **111**, 774-798.
Syono, S., and M. Yamasaki, 1966: Stability of symmetrical motions driven by latent heat release by cumulus convection under the existence of surface friction. *J. Meteor. Soc. Japan.*, **44**, 353-375.
Tuleya, R. E., 1988: A numerical study of the genesis of tropical storms observed during the FGGE year. *Mon. Wea. Rev.*, **116**, 1188-1208.
Tuleya, R. E., and Y. Kurihara, 1981: A numerical study on the effects of environmental flow on tropical storm genesis. *Mon. Wea. Rev.*, **109**, 2487-2506.
Velasco, I., and J. M. Fritsch, 1987: Mesoscale convective complexes in the Americas. *J. Geophys. Res.*, **92**, 9591-9613.
Wang, B., and H. Rui, 1990: Dynamics of the coupled moist Kelvin-Rossby wave on an equatorial β-plane. *J. Atmos. Sci.*, **47**, 397-413.
Webster, P. J., 1983: The large-scale structure of the tropical atmosphere. *Large-Scale Dynamical Processes in the Atmosphere*, B. J. Hoskins and R. P. Pearce (Eds.), Academic Press.
Winn-Nielsen, A., 1993: Studies of CISK. *Atmosfera*, **6**, 51-77.
Xue, Z., and C. J. Neumann, 1984: Frequency and motion of western North Pacific tropical cyclones. Tech. Memo. NWS NHC 23, NOAA, Washington, DC, 80 pp.
Yamasaki, M., 1969: Large-scale disturbances in a conditionally unstable atmosphere in low latitudes. *Papers in Meteor. Geophys.*, **20**, 289-336.
Yamasaki, M., 1988: Towards an understanding of the interaction between convection and the larger-scale in the tropics. *Aust. Meteor. Mag.*, **36**, 171-182.
Yanai, M., 1961: A detailed analysis of typhoon formation. *J. Meteor. Soc. Japan*, **39**, 187- 214.
Yano, J.-I., and K. Emanuel, 1991: An improved model of the equatorial tropopause and its coupling with the stratosphere. *J. Atmos. Sci.*, **48**, 377-389.
Zehr, R. M., 1992: Tropical cyclogenesis in the western North Pacific. NOAA Technical Report NESDIS 61, U.S. Department of Commerce, Washington, DC 20233, 181 pp.
Zehr, R. M., 1993: Recognition of mesoscale vortex initiation as stage one of tropical cyclogenesis. *Preprints, 20th Conf. Hurr. Trop. Meteor.*, San Antonio, TX, Amer. Meteor. Soc., Boston, MA 02108, 405-408.
Zhang, G.-Z., W. Drosdowsky, and N. Nicholls, 1990: Environmental influences on Northwest Pacific tropical cyclone numbers. *Acta Meteorologica Sinica*, **4**, 180-188.